Presynaptic CK2 promotes synapse organization and stability by targeting Ankyrin2

Victoria Bulat,[1,2] Melanie Rast,[1,2] and Jan Pielage[1]

[1]Friedrich Miescher Institute for Biomedical Research, 4058 Basel, Switzerland
[2]University of Basel, 4003 Basel, Switzerland

The precise regulation of synapse maintenance is critical to the development and function of neuronal circuits. Using an in vivo RNAi screen targeting the *Drosophila* kinome and phosphatome, we identify 11 kinases and phosphatases controlling synapse stability by regulating cytoskeletal, phospholipid, or metabolic signaling. We focus on casein kinase 2 (CK2) and demonstrate that the regulatory (β) and catalytic (α) subunits of CK2 are essential for synapse maintenance. CK2α kinase activity is required in the presynaptic motoneuron, and its interaction with CK2β, mediated cooperatively by two N-terminal residues of CK2α, is essential for CK2 holoenzyme complex stability and function in vivo. Using genetic and biochemical approaches we identify Ankyrin2 as a key presynaptic target of CK2 to maintain synapse stability. In addition, CK2 activity controls the subcellular organization of individual synaptic release sites within the presynaptic nerve terminal. Our study identifies phosphorylation of structural synaptic components as a compelling mechanism to actively control the development and longevity of synaptic connections.

Introduction

The function of all neuronal circuits critically depends on appropriate synaptic connectivity. This connectivity is established initially during development and then refined in response to changes in sensory input, information processing, or motor behavior. The execution of innate or learned behavioral programs and the lifelong storage of memories require long-term maintenance of synaptic connectivity, whereas plastic refinement of circuitry is essential to accommodate altered sensory input or incorporate new memory. These two opposing forces of stability and plasticity are evident during development and in mature neuronal circuits (Holtmaat and Svoboda, 2009; Caroni et al., 2012). Despite its importance, it remains unclear whether newly formed synapses are stable by default or whether active mechanisms control synapse stability and longevity (Alvarez and Sabatini, 2007).

To identify regulatory mechanisms controlling synapse stability in vivo, we performed a high-resolution RNAi screen of the *Drosophila* kinome and phosphatome. The *Drosophila* neuromuscular junction (NMJ) allows the analysis of synapse maintenance at the resolution of individual synapses and enabled the identification of essential synapse stability and plasticity genes relevant for neurodegenerative diseases and learning and memory in the past (Jenkins and Bennett, 2001; Eaton et al., 2002; Hafezparast et al., 2003; Eaton and Davis, 2005; Pielage et al., 2005, 2008; Ikeda et al., 2006; Koch et al., 2008; Bednarek and Caroni, 2011; Pielage et al., 2011). We targeted >88% of all kinases and phosphatases encoded in the *Drosophila* genome and identified seven kinases and four phosphatases essential for the maintenance of synaptic connections. This demonstrated that synapse stability is actively controlled and that regulation of the cytoskeleton as well as phospholipid and metabolic signaling represent important signaling nodes. To gain insights into the principles and mechanisms underlying synapse maintenance we focused our analysis on casein kinase 2 (CK2).

CK2 is a serine-threonine kinase composed of two catalytic (CK2α) and two regulatory (CK2β) subunits that form a heterotetrameric α2/β2 holoenzyme (Meggio and Pinna, 2003). CK2 has been suggested as a potential regulator of neuronal development and function (Charriaut-Marlangue et al., 1991; Blanquet, 2000) but the severe neurodevelopmental phenotypes and early embryonic lethality of *CK2α* and *CK2β* knockout

Correspondence to Jan Pielage: jan.pielage@fmi.ch

Abbreviations used in this paper: Ank2-L, Ankyrin2-L; Brp, Bruchpilot; CK2, casein kinase 2; Dlg, Discs-large; FasII, Fasciclin II; IP, immunoprecipitation; MARCM, mosaic analysis with a repressible cell marker; mbu, mushroom body undersized; Mts, microtubule star; NMJ, neuromuscular junction; Nrg, Neuroglian; VDRC, Vienna Drosophila RNAi Center.

The Rockefeller University Press $30.00
J. Cell Biol. Vol. 204 No. 1 77–94
www.jcb.org/cgi/doi/10.1083/jcb.201305134

mice thus far prevented an analysis of CK2 in postmitotic neurons using loss-of-function mutations (Buchou et al., 2003; Lou et al., 2008; Seldin et al., 2008; Huillard et al., 2010). Knockdown or inhibitor-based approaches identified first roles in postsynaptic neurotransmitter receptor control and organization of ion channel distribution to specialized neuronal membrane domains (Chung et al., 2004; Cheusova et al., 2006; Bréchet et al., 2008; Brachet et al., 2010; Sanz-Clemente et al., 2010). The molecular mechanisms controlling CK2 assembly, regulation, or potential independent functions of the individual subunits in neurons in vivo remain unclear.

The *Drosophila* genome encodes a catalytic CK2α subunit, a regulatory subunit CK2β, and two testis-specific CK2β subunits (CK2β′ and CK2βtes) but lacks the alternative catalytic CK2α′ subunit required for germ line development in vertebrates (Blanquet, 2000). CK2α and CK2β share >88% sequence identity with human CK2α and CK2β (Saxena et al., 1987) and, given that null mutations die at embryonic/early larval stages, are essential for *Drosophila* development (this paper; Jauch et al., 2002; Lin et al., 2002). Using dominant-negative and hypomorphic mutations, it has been demonstrated that individual subunits of CK2 contribute to circadian clock regulation, photoreceptor targeting, and proliferation of mushroom body neurons, but no loss-of-function study has yet addressed potential synaptic roles of CK2 (Jauch et al., 2002; Lin et al., 2002; Akten et al., 2003; Berger et al., 2008).

Here, we identified essential functions of CK2α and CK2β in synapse maintenance by using conditional analyses of loss-of-function alleles and in vivo rescue assays. The combination of these approaches with biochemical assays enabled us to dissect the molecular mechanisms controlling CK2 complex formation and function during synapse maintenance in vivo. We identified CK2-dependent regulation of a presynaptic stability network linking synaptic cell adhesion molecules via a giant Ankyrin to microtubules as a novel mechanism to actively control synapse development and maintenance.

Results

RNAi screen identifies kinases and phosphatases essential for synapse stability

To identify regulatory mechanisms controlling the maintenance of synaptic connections, we performed an in vivo RNAi-based screen of the *Drosophila* kinome and phosphatome. At the *Drosophila* NMJ, synapse stability can be assessed at the resolution of individual synapses by monitoring the apposition of pre- and postsynaptic markers. In wild-type animals the presynaptic active zone marker Bruchpilot (Brp) is always found in precise apposition to postsynaptic glutamate receptor clusters, and synapse retractions occur at very low frequency (≤5% of all NMJs). In contrast, knockdown or mutation of genes essential for synaptic maintenance results in a significant increase in synaptic retractions characterized by a loss of Brp and a fragmentation of the presynaptic motoneuron membrane despite persisting postsynaptic glutamate receptor clusters (Wodarz et al., 1995; Eaton et al., 2002; Pielage et al., 2005, 2008, 2011; Koch et al., 2008). Thus, this in vivo assay allows a systematic and unbiased identification of novel regulators of synapse stability.

We identified 389 transgenic RNAi lines (Vienna Drosophila RNAi Center [VDRC] RNAi collection; Dietzl et al., 2007) targeting 223 kinases and 125 phosphatases, including their regulatory subunits, that represent >88% of the entire *Drosophila* kinome and phosphatome (Table S1). We expressed transgenic double-stranded RNA (dsRNA) constructs in presynaptic motoneurons (*elav*-GAL4; UAS-*dcr2* at 27°C) and monitored synapse stability using our high-resolution immunohistochemical assay. The knockdown of 11 kinases and phosphatases resulted in a significant increase in synapse retractions (Fig. 1). We verified these results using independent dsRNA lines (VDRC or TRiP, Bloomington Stock Center) for four candidates, demonstrating that the observed effects were caused by specific knockdown of the target gene (Fig. 1 G, Fig. S1 G, and Table S2). The severity ranged from small retractions affecting only distal boutons (Fig. 1 E and Fig. S1 F) to large retraction encompassing entire NMJ branches (Fig. 1, C, D, and F; and Fig. S1, B, C, and E) to complete eliminations of the entire presynaptic nerve terminal (Fig. 1 B and Fig. S1 D). The analysis of synaptic retractions on ventral, medial, and dorsal muscle groups revealed significant differences in synaptic retraction frequencies between muscle groups (Fig. 1 G, Fig. S1 G, and Table S2). To ensure that the observed phenotypes represented de facto synaptic retractions and not simply aberrant localization of presynaptic Brp, we analyzed all genotypes with the presynaptic vesicle marker Synapsin (Syn) and postsynaptic Discs-large (Dlg). We observed qualitatively and quantitatively similar phenotypes for all genotypes (Fig. S2). Thus, our screen successfully identified kinases and phosphatases that are required presynaptically to maintain synaptic connections. To elucidate the cellular mechanisms underlying regulation of synapse stability, we focused on the β subunit of CK2β, as knockdown of *CK2β* resulted in one of the most severe phenotypes identified in our screen (Fig. 1 G). Despite the clear importance of CK2 for nervous system development and function (Buchou et al., 2003; Lou et al., 2008; Seldin et al., 2008; Huillard et al., 2010; Sanz-Clemente et al., 2010), potential presynaptic functions have not yet been addressed in any system.

Presynaptic CK2β is essential for synapse stability

We first tested whether CK2β is required not only pre- but also postsynaptically for synapse maintenance. Presynaptic knockdown resulted in synaptic retractions at up to 50% of NMJs depending on the muscle group analyzed (Fig. 2, B and G; and Table S2). Retraction severity ranged from small retractions affecting 1–2 distal boutons to large retractions affecting the entire nerve terminal (Fig. 2 H). In contrast, knockdown in the postsynaptic muscle did not significantly increase retraction frequency or severity (Fig. 2, C, G, and H). To control for the specificity of our RNAi-mediated knockdown, we generated an antibody against CK2β. This antibody specifically recognizes CK2β on Western blots of larval brain extracts but does not recognize CK2β in situ. Neuronal- but not muscle-specific expression of CK2β RNAi caused an efficient knockdown of

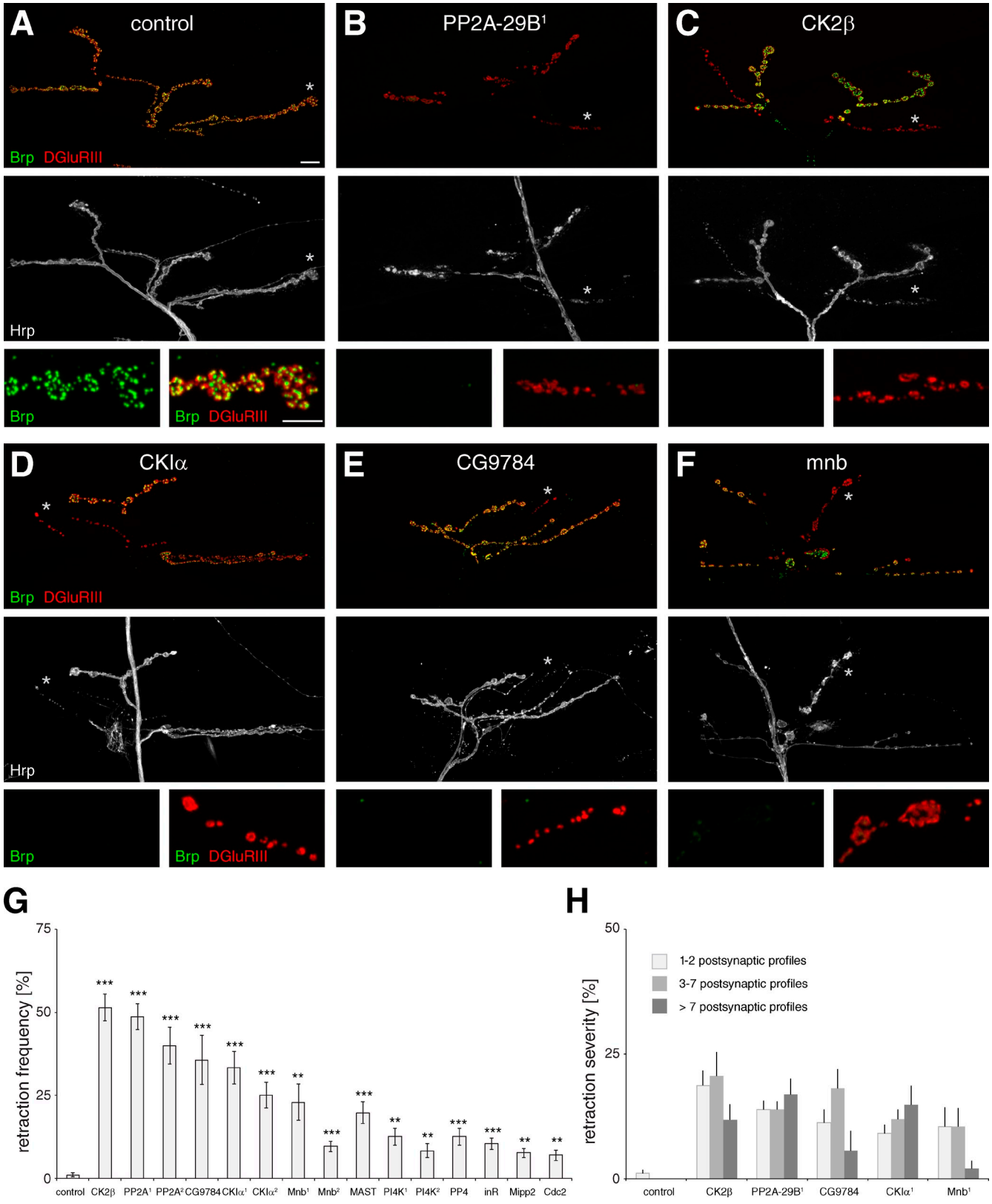

Figure 1. **RNAi screen identifies kinases and phosphatases essential for synapse stability.** (A–F) NMJs on muscles 1/9 and 2/10 were stained for the presynaptic active zone marker Brp (green), postsynaptic glutamate receptors (DGluRIII, red), and the presynaptic membrane marker Hrp (white). (A) A stable wild-type NMJ on muscles 1/9. (B–F) RNAi-mediated knockdown of the indicated kinases or phosphatases caused synaptic retractions that ranged from a few unopposed postsynaptic profiles (E) to the elimination of all presynaptic markers (B). Asterisks indicate regions shown at high magnification. (G) Quantification of synaptic retraction frequencies (**, $P \leq 0.01$; ***, $P \leq 0.001$; $n = 9–15$ animals, muscles 1/9 and 2/10). Two independent RNAi lines were analyzed when available (PP2A, CKIα, Mnb, and PI4K). (H) Quantification of synaptic retraction severity. Bars: (main panels) 10 µm; (enlarged panels below) 5 µm. Error bars represent SEM.

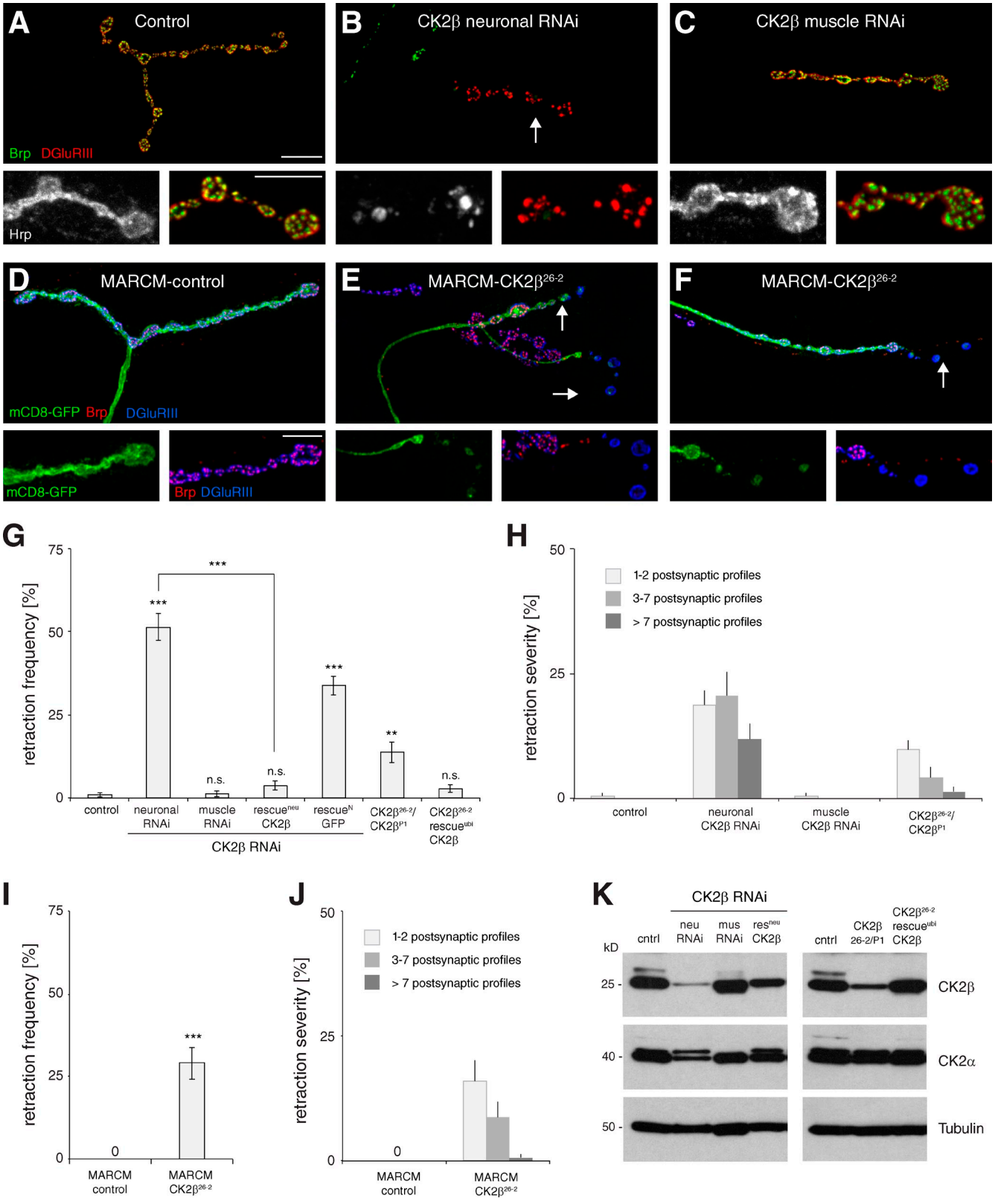

Figure 2. **Presynaptic CK2β is essential for synapse stability.** (A) A stable wild-type NMJ on muscle 4. (B) Loss of presynaptic CK2β caused severe synaptic retractions. (C) Knockdown of muscle CK2β did not impair synapse stability. (D–F) MARCM-based analyses of control and *CK2β*-null mutant motoneurons (arrows). MARCM motoneurons are marked by the expression of membrane-bound GFP (mCD8-GFP, green). (D) Stable control NMJ. (E and F) $CK2\beta^{26\text{-}2}$ mutant motoneurons. Synaptic retractions were evident at distal areas of the mutant nerve terminals, characterized by a loss of presynaptic Brp and fragmentation of the MARCM membrane marker opposite postsynaptic glutamate receptor clusters (arrows). Bars: (main panels) 10 µm; (enlarged panels below) 5 µm. (G) Quantification of synaptic retraction frequency. n.s., not significant. (H) Quantification of synaptic retraction severity (**, $P \leq 0.01$; ***, $P \leq 0.001$; n = 9–13 animals, muscles 1/9 and 2/10 for G and H). (I and J) Quantification of synaptic retraction frequency (I) and severity (J) of

CK2β protein levels in larval brain extracts (Fig. 2 K) that could be rescued by coexpression of CK2β (see Materials and methods for generation of UAS-*CK2β*) but not of membrane-bound GFP (mCD8-GFP). To complement the RNAi-based results, we next analyzed mutations in *CK2β* (*mushroom body undersized*; *mbu*) that were previously identified as regulators of mushroom body neuron proliferation and circadian rhythm (Jauch et al., 2002; Akten et al., 2003). Although the hypomorphic $CK2\beta^{P1}$ (mbu^{P1}) mutation is adult viable, the null allele $CK2\beta^{26\text{-}2}$ ($mbu^{26\text{-}2}$) is lethal at the first/second instar larval stage. Transheterozygous $CK2\beta^{P1}/CK2\beta^{26\text{-}2}$ mutant larvae showed a small but significant increase in synaptic retractions (Fig. 2, G and H). The quantitative differences compared with the RNAi-evoked phenotypes are likely caused by the lower reduction of neuronal CK2β protein levels (Fig. 2 K). Consistently, transheterozygous $CK2\beta^{P1}/CK2\beta^{26\text{-}2}$ animals survived to adulthood, whereas neuronal knockdown of CK2β caused pupal lethality. We next applied the mosaic analysis with a repressible cell marker (MARCM) technique to generate *CK2β*-null mutant motoneurons (Lee and Luo, 1999). In mCD8-GFP–marked control clones we did not observe any impairment of synapse stability (Fig. 2, D, I, and J). In contrast, loss of *CK2β* ($CK2\beta^{26\text{-}2}$ MARCM) caused synaptic retraction at 33% of the mutant NMJs characterized by a loss of presynaptic Brp and a fragmentation of the mCD8-GFP membrane marker despite persisting glutamate receptor clusters (Fig. 2, E, F, I, and J). This rate is in accordance with our RNAi-based results, as *CK2β* knockdown caused synaptic retractions at 18–51% of NMJs depending on the analyzed muscle group (Table S2). Furthermore, we were able to rescue the lethality and synaptic retraction phenotype and to restore CK2β protein levels of $CK2\beta^{26\text{-}2}$ null mutant animals by ubiquitous expression of *CK2β* (Fig. 2, G and K). Together, our data demonstrate that presynaptic CK2β is essential for the maintenance of synaptic connections.

Presynaptic CK2α is essential for synapse stability

CK2β encodes the regulatory subunit of the CK2 holoenzyme, which is composed of two catalytic CK2α and two CK2β subunits (α2/β2). Thus, we next analyzed whether CK2α is also required for synapse stability (*CK2α* RNAi lines were not available from the VDRC and thus we did not identify *CK2α* in our screen). Mutations in *CK2α* were previously identified in genetic screens for axon guidance in the optic lobe ($CK2\alpha^{H3091}$, $CK2\alpha^{G703}$; Berger et al., 2008) and for regulators of circadian rhythm ($CK2\alpha^{Tik}$, $CK2\alpha^{TikR}$; see Materials and methods; Fig. S3 A; Lin et al., 2002; Berger et al., 2008). However, the consequences of strong loss-of-function mutations for nervous system or synapse development have not been analyzed so far. Here, we identified two PiggyBac insertions ($CK2\alpha^{P1}$, $CK2\alpha^{P2}$; splice-acceptor mutations generated in Schuldiner et al., 2008; www.flybase.org) as potential alleles of *CK2α* (Fig. S3 A). Complementation analyses demonstrated that all alleles are mutations of *CK2α* (Table S2). Although homozygous $CK2\alpha^{P2}$ and $CK2\alpha^{TikR}$ mutations resulted in embryonic lethality, animals homozygous for $CK2\alpha^{P1}$ and transheterozygous combinations survived up to pupal stages except for $CK2\alpha^{P2/TikR}$ (Table S2). Based on their lethality phase, we placed the mutations into the following allelic series ($CK2\alpha^{P2} = CK2\alpha^{TikR} > CK2\alpha^{P1} \geq CK2\alpha^{Tik} > CK2\alpha^{H3091} \geq CK2\alpha^{G703}$; Table S2), which correlates well with the molecular nature of the alleles (Fig. S3 A). Importantly, all allelic combinations caused a significant increase in the frequency of synaptic retractions (Fig. 3, A–C and G; and Fig. S3, B and C). We observed slightly weaker phenotypes on ventral (muscles 6 and 7) than on dorsal muscle groups (muscles 1, 2, 9, and 10); however, the relative phenotypic strength of the different allelic combinations remained identical, with the highest synaptic retraction frequencies observed for strong allelic combinations surviving to late larval stages (Fig. S3, B and C; and Table S2).

To analyze potential tissue-specific functions of CK2α, we generated a UAS construct allowing directed expression of wild-type CK2α. To address the requirements of CK2α kinase activity, we generated a kinase-dead version of CK2α ($CK2\alpha^{KD}$) by mutating lysine 66 to methionine (K66M), mimicking the in vitro characterized kinase-dead mutation of human CK2α (Fig. 4 A; Penner et al., 1997). We used phi-c31–mediated site-specific integration into the attP40 landing site for all transgenic constructs throughout this study to ensure equal expression levels (Bischof et al., 2007). In addition, we generated a CK2α-specific antibody. Ubiquitous expression of CK2α (*da*-Gal4) rescued the lethality of all transheterozygous combinations and of homozygous $CK2\alpha^{P1}$ and $CK2\alpha^{P2}$ mutant animals, demonstrating the specificity of all mutations (Fig. 3 G, Table S2, and unpublished data). Importantly, pre- but not postsynaptic expression of CK2α was sufficient to rescue synapse stability and to restore neuronal CK2α protein levels in all analyzed combinations (Fig. 3, D, E, G, and H). Because of the proximity of CK2α to the centromere we were unable to analyze the strong loss-of-function mutation $CK2\alpha^{P2}$ using MARCM. To circumvent the embryonic lethality we rescued $CK2\alpha^{P2}$ mutants by ubiquitous expression of *CK2α*, while at the same time preventing neuronal expression (*da*-Gal4; *elav*-Gal80). We observed synaptic retractions at 43% of analyzed NMJs in these animals, which is in accordance with our analysis of transheterozygous combinations (Fig. 3 G). CK2α kinase activity is essential for synapse stability, as presynaptic expression of $CK2\alpha^{KD}$ was not sufficient to rescue synaptic retractions, despite being expressed at levels similar to wild-type CK2α (Fig. 3, F–H). In addition, ubiquitous expression of $CK2\alpha^{KD}$ did not rescue lethality associated with *CK2α* mutations. Thus, we conclude that presynaptic CK2α kinase activity is required for maintenance of the presynaptic nerve terminal.

MARCM control and $CK2\beta^{26\text{-}2}$ mutant motoneurons (n = 17–33 animals). (K) Western blot analysis of CK2β, CK2α, and tubulin protein levels in larval brain extracts of the genotypes analyzed in G. Neuronal knockdown of CK2β led to a severe reduction in CK2β and a modest reduction in CK2α protein levels. CK2β and CK2α levels were rescued by neuronal coexpression of wild-type CK2β. Brain extracts of $CK2\beta^{P1/26\text{-}2}$ mutants showed slightly reduced CK2β and normal CK2α protein levels. $CK2\beta^{26\text{-}2}$ mutant animals rescued by ubiquitous expression of CK2β had wild type–like CK2α and CK2β protein levels. Error bars represent SEM.

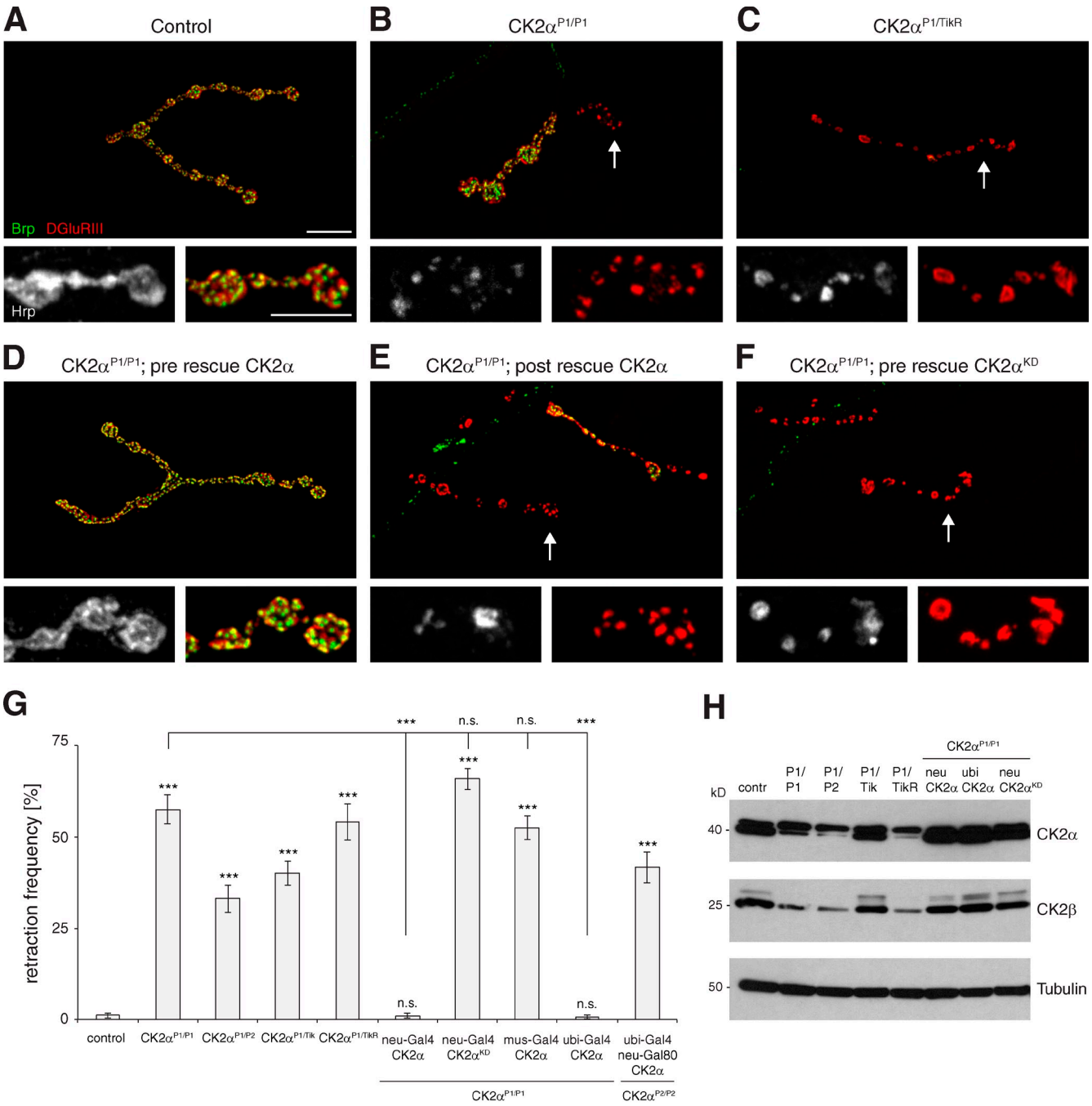

Figure 3. **Presynaptic CK2α is essential for synapse stability.** (A) A stable wild-type NMJ on muscle 4. (B and C) Mutations in *CK2α* resulted in synaptic retractions ranging between loss of few terminal boutons (B, arrow) and complete eliminations of the NMJ (C, arrow). (D–E) Neuronal but not muscle-specific expression of wild-type CK2α rescued the synaptic retraction phenotype in *CK2α* mutant animals. Large synaptic retractions were still evident after postsynaptic expression (E, arrow). (F) Neuronal expression of a kinase-dead version of CK2α was not sufficient to restore synapse stability (arrow). Bars: (main panels) 10 µm; (panels below) 5 µm. (G) Quantification of synaptic retraction frequencies of different allelic combinations and tissue-specific rescues on muscles 1/9 and 2/10 (***, $P \leq 0.001$; $n = 9–22$ animals). n.s., not significant. (H) Western blot analysis of larval brain extracts demonstrated a strong reduction in CK2α protein levels in $CK2\alpha^{P1/P1}$, $CK2\alpha^{P1/P2}$, and $CK2\alpha^{P1/TikR}$ but not in $CK2\alpha^{P1/Tik}$ mutant animals (the lower band corresponds to CK2α protein). A corresponding decrease in CK2β protein levels was observed. CK2α and CK2β proteins levels were efficiently restored by neuronal or ubiquitous expression of either wild-type or kinase-dead CK2α. Error bars represent SEM.

CK2α–CK2β interaction is essential for the control of synapse stability

In vitro, CK2α has the ability to phosphorylate CK2 targets independently of CK2β (Hériché et al., 1997; Litchfield, 2003); however, because of the high stability of the complex it has been suggested that CK2 may act primarily as a α2/β2 holoenzyme in vivo (Salvi et al., 2006; Niefind et al., 2009). In support of such a hypothesis, we observed a reduction in CK2β protein levels in larval brain extracts for CK2α mutations that reduce CK2α protein levels ($CK2\alpha^{P1}$, $CK2\alpha^{P2}$, and $CK2\alpha^{TikR}$) but not for mutations impairing only CK2α activity ($CK2\alpha^{Tik}$; Fig. 3 H). We were able to restore CK2β levels by expression of wild-type or

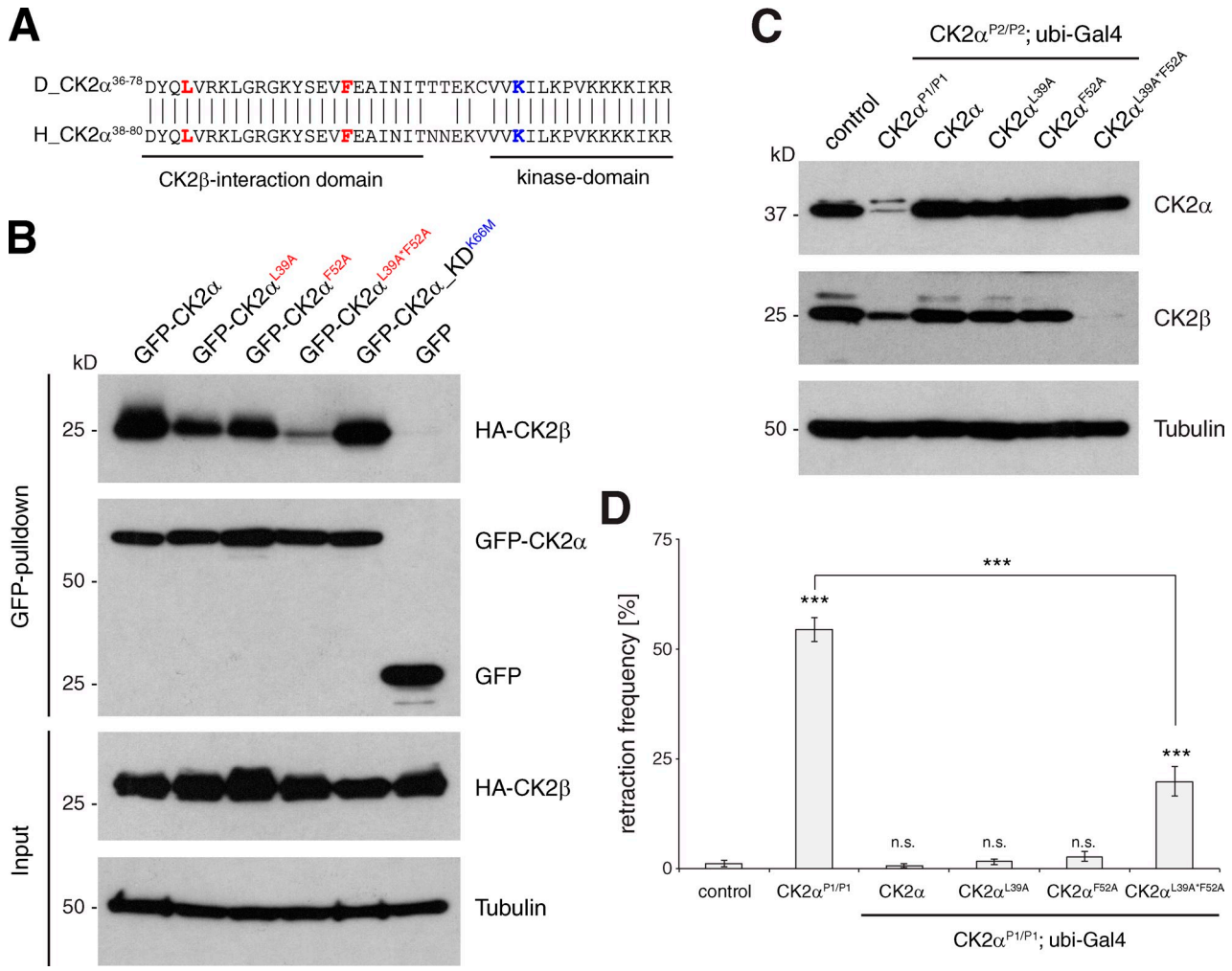

Figure 4. **CK2α–CK2β interaction is essential for the control of synapse stability.** (A) Sequence comparison of *Drosophila* and human CK2α. Residues required for the CK2α–CK2β interaction (leucine 39 and phenylalanine 52 in *Drosophila*) are marked in red. Lysine 66 that is essential for CK2α kinase function is marked in blue. (B) S2 cell IP assay analyzing the CK2α–CK2β interaction. HA-tagged CK2β was efficiently precipitated by GFP-tagged wild-type or kinase-dead CK2α. The mutations CK2α^{L39A} and CK2α^{F52A} reduced the efficiency of the IP. The double mutant CK2α^{L39A*F52A} caused a further reduction of the interaction. No pull-down was observed in the GFP control. (C) Western blot analysis of larval brain extracts demonstrated that ubiquitous expression of wild-type CK2α, CK2α^{L39A}, or CK2α^{F52A} in *CK2α$^{P2/P2}$*-null animals efficiently restored CK2α and CK2β protein levels. In contrast, expression of CK2α^{L39A*F52A} restored CK2α levels, but failed to rescue the reduction in CK2β protein levels. (D) Quantification of synaptic retraction frequencies (***, P ≤ 0.001, *n* = 12–17 animals, muscles 1/9 and 2/10). n.s., not significant. Error bars represent SEM.

kinase-dead CK2α, further demonstrating that CK2α abundance but not kinase activity controls CK2β protein levels in vivo (Fig. 3 H). Similarly, presynaptic knockdown of *CK2β* resulted in a reduction in CK2α levels (Fig. 2 K). These results indicate that direct interaction between the two subunits is essential for CK2 complex stability in vivo. We next aimed to directly test the requirement of the CK2α–CK2β interaction for synapse stability.

A recent biochemical study of human CK2 identified two CK2α residues that are independently required for the association with CK2β in vitro but that do not affect kinase activity (L41, F54; Raaf et al., 2011). These residues are conserved in *Drosophila* CK2α (L39, F52; Fig. 4 A). We first examined whether alanine substitution of these residues disrupted the CK2α–CK2β interaction in immunoprecipitation (IP) assays using *Drosophila* S2 cell extracts. GFP-tagged wild-type CK2α efficiently precipitated HA-tagged CK2β but single-point mutations (L39A or F52A) reduced and the double mutation (L39A*F52A) almost completely abolished the CK2α–CK2β interaction (Fig. 4 B). Consistent with our in vivo data (Fig. 3 H), the kinase-dead mutation (K66M) did not impair this interaction (Fig. 4 B). We then generated transgenic flies carrying either single mutations or the double mutation and expressed the mutated versions of CK2α ubiquitously in the background of the strong *CK2α^{P2}* mutation. The site-specific integration of all constructs ensured identical expression levels (Fig. 4 C). Surprisingly, expression of CK2α^{L39A} and CK2α^{F52A}, which caused a strong reduction of the CK2β interaction in vitro, fully restored CK2β levels and, thus, did not impair the CK2α–CK2β interaction in vivo (Fig. 4 C). In contrast, CK2α^{L39A*F52A} completely failed to restore CK2β protein despite the presence of equivalent CK2α protein levels (Fig. 4 C). We next tested the ability of these constructs to rescue synapse retractions of *CK2α* mutant animals. Both single mutations completely rescued synapse stability phenotypes and lethality of *CK2α* mutants. In contrast,

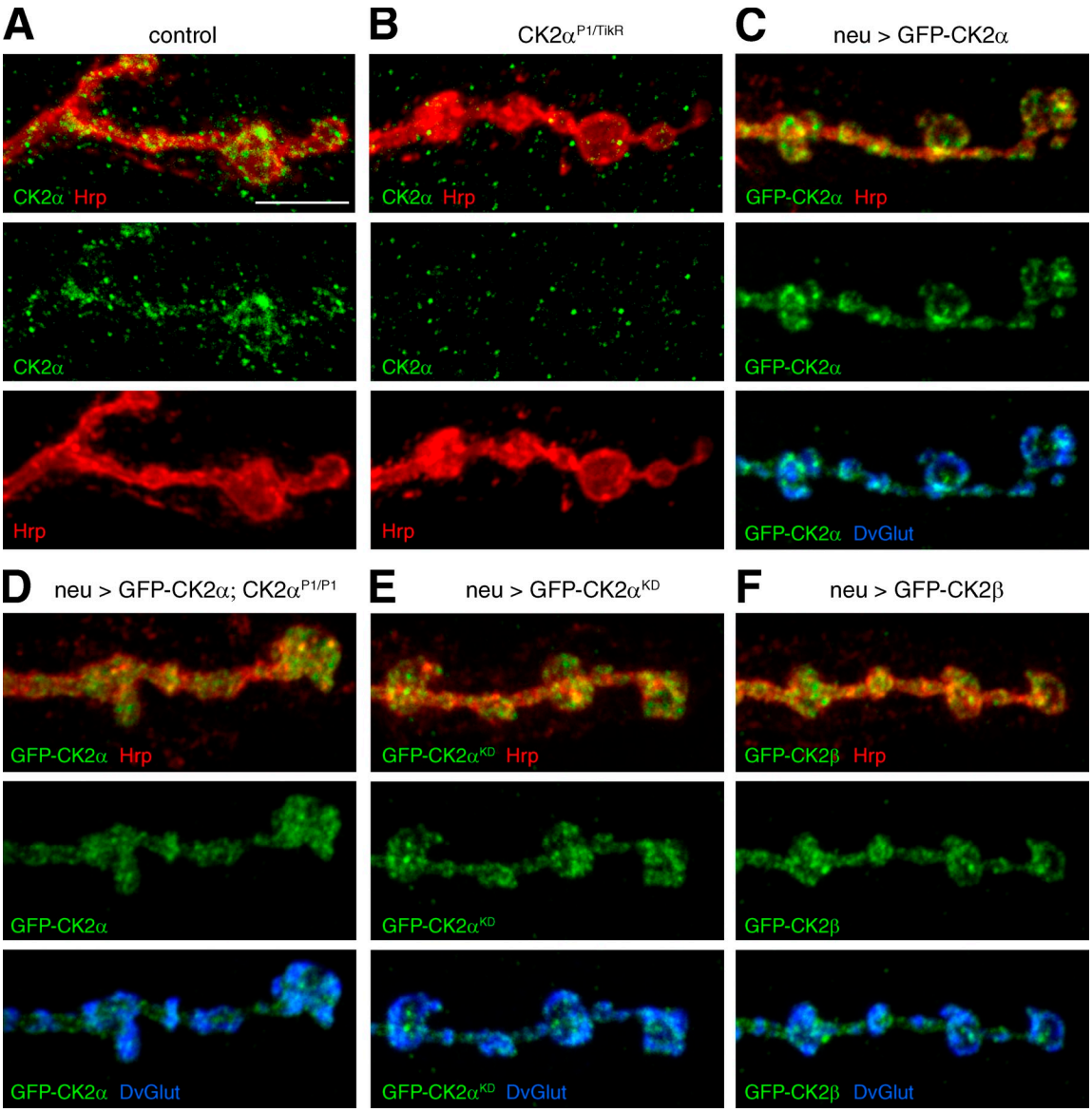

Figure 5. **CK2α and CK2β localize to the presynaptic nerve terminal.** (A and B) Analysis of endogenous CK2α localization. CK2α (green) is present within the presynaptic nerve terminal marked by Hrp (red; A). In *CK2α*$^{P1/TikR}$ mutant animals presynaptic CK2α staining is absent (B). (C–F) Analysis of the synaptic localization of GFP-tagged CK2α and CK2β. (C) GFP-tagged wild-type CK2α (green) localized to synaptic bouton and interbouton regions marked by the synaptic vesicle marker DvGlut (blue). (D) A comparable distribution was observed when GFP-CK2α was expressed in *CK2α* mutant animals. GFP-tagged CK2α completely restored synapse stability in these animals, indicating functional distribution. (E) Presynaptic CK2α localization did not depend on kinase activity. (F) Neuronal expression of GFP-tagged CK2β (green) resulted in a similar presynaptic localization. Bar, 5 µm.

CK2α^{L39A*F52A} only partially rescued the retraction phenotype and slightly improved viability (lethality phase shift from first to third instar larval stage). Together, our data demonstrate that L39 and F52 cooperatively mediate the interaction between CK2α and CK2β in vivo and that this interaction is essential for synapse stability and animal viability.

We next addressed the localization of CK2α and CK2β at the NMJ. While the CK2α and CK2β antibodies generated in this study did not work in situ, a peptide antibody generated against aa 68–87 of CK2α (Acris) recognized CK2α protein at wild-type NMJs. CK2α is present within presynaptic boutons defined by the motoneuron membrane marker Hrp (Fig. 5 A). This presynaptic staining is completely absent in *CK2α*$^{P1/TikR}$ mutant animals, demonstrating the specificity of antibody (Fig. 5 B). To further verify the presynaptic localization of CK2 we generated UAS-GFP–tagged versions of CK2α and CK2β. Expression of GFP-CK2α and GFP-CK2β in motoneurons resulted in presynaptic localization similar to endogenous CK2α (Fig. 5, C and F). Importantly, expression of GFP-tagged CK2α in *CK2α* mutant animals completely rescued synaptic retractions and lethality (Table S2 and Fig. 5 D). The synaptic localization of CK2α did not depend on kinase activity (Fig. 5 E).

CK2 controls synapse stability independently of PP2A

Although our data indicate that CK2 functions mainly as a CK2α–CK2β holoenzyme, the improvement of synapse stability in the CK2α^{L39A*F52A} rescue suggested possible CK2β-independent

activity of CK2α. It has been demonstrated that CK2α can directly bind and activate the protein phosphatase PP2A in the absence of CK2β (Hériché et al., 1997). Interestingly, the structural subunit PP2A-29B was a strong hit in our screen, and a CK2α-specific residue required for this interaction (E165) is mutated in the $CK2\alpha^{Tik}$ allele (Fig. S4 A; $CK2\alpha^{Tik}$ carries an additional mutation near the ATP-binding pocket [M161K]; Lin et al., 2002). Prior analysis of PP2A function at the NMJ, using expression of a dominant-negative version of the catalytic subunit microtubule star (dnMts), demonstrated a requirement of PP2A for synapse formation (Viquez et al., 2009). To address a potential interaction between CK2 and PP2A, we first confirmed the requirement of PP2A by RNAi and by expressing dnMts. We observed a significant increase in synaptic retractions in all cases (Fig. S4, C–E; Fig. S1, B and G; Fig. S2 B; and Table S2) and could confirm the previously reported defects in synapse formation (Fig. S4, G and H). To test whether a CK2α–PP2A interaction is required for the control of synapse maintenance, we generated a series of mutations in the PP2A interaction domain by mutating only E165 ($CK2\alpha^{E165A}$) or all three essential PP2A interaction site residues to alanine ($CK2\alpha^{ENRK165ANAA}$), thereby completely abolishing the CK2α–PP2A interaction (Hériché et al., 1997; Fig. S4 A). In addition, we mimicked the two individual mutations of the $CK2\alpha^{Tik}$ allele ($CK2\alpha^{M161K}$, $CK2\alpha^{E165D}$). Surprisingly, the CK2α–PP2A interaction was not essential for synapse maintenance as all mutations affecting the PP2A interaction site completely rescued the synaptic retraction phenotype of *CK2α* mutants (Fig. S4 F). In contrast, $CK2\alpha^{M161K}$ failed to rescue the synaptic retraction phenotype and the lethality of *CK2α* mutant animals (Fig. S4 F), which indicates that introduction of a charged amino acid into the ATP-binding domain severely impairs CK2α activity. Our data demonstrate that direct interaction of CK2α and PP2A is not essential for the regulation of synapse stability.

CK2 maintains the synaptic localization of synapse stabilizing proteins

Next we aimed to identify the cellular targets that depend on CK2 activity to control synapse stability. In a candidate approach, we analyzed cell adhesion and cytoskeletal proteins that have previously been identified as CK2 targets or that have been implicated in the control of synapse stability. These molecules included the NCAM homologue Fasciclin II (FasII), the L1-type CAM Neuroglian (Nrg), and the adaptor molecule Ankyrin2-L (Ank2-L; Schuster et al., 1996; Wong et al., 1996; Koch et al., 2008; Pielage et al., 2008; Enneking et al., 2013). We hypothesized that the synaptic localization of CK2 targets that cause the synapse stability defects should already be altered at NMJs that do not yet show signs of instability. In CK2α mutants we observed a striking reduction in Nrg180 and Ank2-L levels, especially at distal boutons of the NMJ. Importantly, at these terminals we did not observe any alteration in the distrubution of the synaptic vesicle marker DvGlut, a highly sensitive marker of synapse disassembly. The reduction in Nrg180 and Ank2-L levels was most severe at distal boutons but significant throughout the entire nerve terminal (Fig. 6, A, B, D, E, and G–I) at all NMJs analyzed. In contrast, we did not observe any alteration of FasII levels at these NMJs (Fig. 6 J). Importantly, presynaptic expression of wild-type but not of kinase-dead CK2α was sufficient to restore Nrg180 and Ank2-L levels in all synaptic boutons (Fig. 6, G and H). Western blot analysis of larval brain extracts demonstrated no obvious alterations in Nrg180 and only small reductions in Ank2-L protein levels in *CK2α* mutants, which suggests that CK2 activity mainly controls synaptic localization (Fig. 6 K). We previously identified Ank2-L as an adaptor protein controlling synapse stability by linking the microtubule cytoskeleton to the presynaptic membrane (Pielage et al., 2008). Indeed, we observed a significant decrease of the microtubule-associated protein Futsch (MAP1b homologue) within the presynaptic terminal that could be rescued by expression of wild-type but not kinase-dead CK2α (Table S2). Vertebrate L1 CAM is a direct target of CK2α (Wong et al., 1996), and *Drosophila* Nrg180 is essential for synapse maintenance (Enneking et al., 2013); therefore, we tested whether UAS-Gal4–mediated expression of Nrg180 in CK2α mutant animals is sufficient to restore presynaptic Nrg180 levels and synapse stability. Although expression of Nrg180 restored presynaptic Nrg180 levels in CK2α mutant animals (Fig. 6, C and G), it failed to rescue the impairment in synapse stability (Fig. 6 L). Consistently, this ectopic increase in presynaptic Nrg180 levels was not sufficient to restore presynaptic Ank2-L levels (Fig. 6, F and H).

CK2 controls synaptic stability via Ank2-L

If phosphorylation of Ank2-L is indeed essential to the control of synapse stability, overexpression of presynaptic CK2α may alleviate synaptic retractions caused by a partial loss of Ank2-L. The hypomorphic *ank2-L* allele $ank2^{f02001}$ (abbreviated $ank2^{P2}$) is a PiggyBac insertion in the *ank2-L* isoform–specific exon resulting in a truncation of the Ank2-L protein after aa 2518 (Ank2-L: 4083 aa, www.flybase.org). This mutation causes a significant increase in synaptic retractions compared with controls (Fig. 7, A, B, E, and F; Pielage et al., 2008). Indeed, presynaptic expression of CK2α in $ank2^{P2/P2}$ mutant animals significantly alleviated the synaptic retraction phenotype (Fig. 7, C, E, and F), whereas expression of $CK2\alpha^{KD}$ further enhanced the synaptic retraction phenotypes (Fig. 7, D–F). This rescue is likely caused by a modulation of residual activity of the truncated Ank2-L protein, as we were unable to improve the synaptic retraction phenotype of $ank2^{P1/P1}$ ($ank2^{f00518}$; Pielage et al., 2008)-null mutant animals that lack all Ank2 protein by presynaptic expression of CK2α (Fig. 7, G and H). To further validate these results we performed genetic interaction experiments. Removal of one copy of *CK2α* in $ank2^{P2/P2}$ mutant animals or removal of one copy of *ank2* in $CK2\alpha^{P1/P1}$ mutant animals significantly increased the frequency of synaptic retractions (Fig. 7, I and J). Together, these results identify Ank2-L as a potential direct target of CK2 in vivo. We next analyzed the Ank2-L open reading frame for potential CK2 phosphorylation sites using the web tool KinasePhos (Huang et al., 2005). The KinasePhos program identified up to 135 serine residues and 48 threonine residues as potential CK2 phosphorylation sites within the Ank2-L protein sequence (cut-off set to > -6). We focused our biochemical analysis on a C-terminal domain ($Ank2\text{-}L^{C}$ = aa 3134–3728) and the central microtubule-binding domain ($Ank2^{MT}$ = aa 1682–2089), as these domains

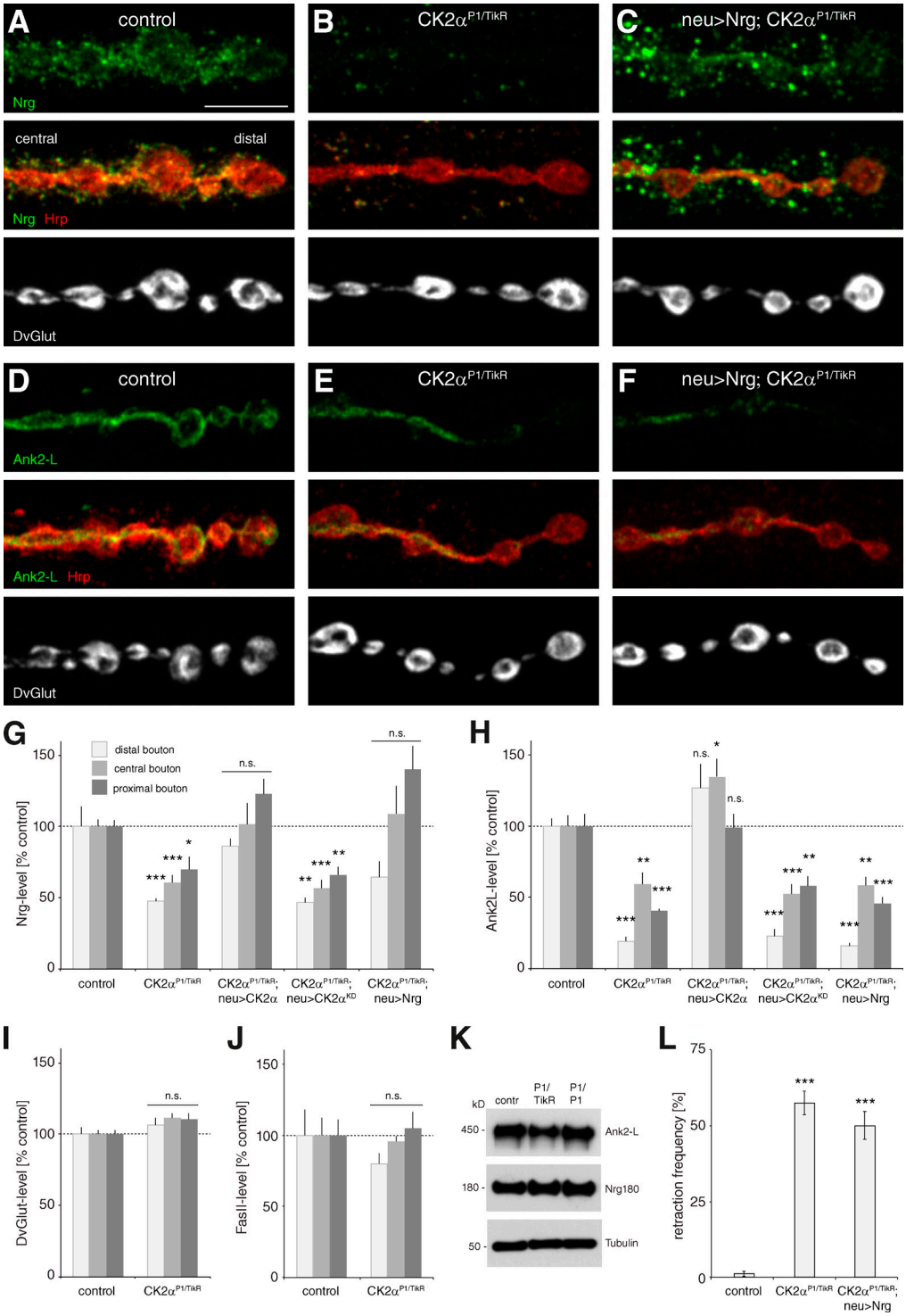

Figure 6. **CK2 maintains the synaptic localization of cytoskeletal proteins.** (A–C) Analysis of Nrg distribution at muscle 4 NMJs. The presence of DvGlut in distal boutons and an intact presynaptic membrane indicate stable nerve terminals. (A) At wild-type NMJs, Nrg was present in all synaptic boutons colocalizing with the membrane marker Hrp. (B) At *CK2α*$^{P1/TikR}$ mutant NMJs, Nrg levels were significantly reduced throughout the presynaptic nerve terminal and especially at distal boutons. (C) Neuronal expression of Nrg in *CK2α*$^{P1/TikR}$ mutants significantly increased presynaptic Nrg levels. (D–F) Analysis of Ank2-L distribution at muscle 4 NMJs. (D) At wild-type NMJs, Ank2-L was present uniformly throughout the presynaptic nerve terminal. (E) At *CK2α*$^{P1/TikR}$ mutant NMJs, Ank2-L staining intensities were significantly reduced, especially at the most distal boutons. (F) Neuronal expression of Nrg in *CK2α*$^{P1/TikR}$ mutants was not sufficient to restore presynaptic Ank2-L levels. Bars, 5 µm. (G–J) Quantification of presynaptic Nrg (G), Ank2-L (H), DvGlut (I), and FasII (J) protein levels at distal, central, and proximal boutons. Presynaptic expression of wild-type CK2α, but not of kinase-dead CK2α, was sufficient to restore Nrg and Ank2-L levels. Expression of Nrg in the *CK2α*$^{P1/TikR}$ mutant significantly increased Nrg but not Ank2-L levels. Presynaptic levels of DvGlut or FasII were not significantly altered in *CK2α*$^{P1/TikR}$ mutant animals (*, $P \leq 0.05$; **, $P \leq 0.01$; ***, $P \leq 0.001$; segment A4, muscle 4, $n = 6–12$ NMJs). (K) Western blot analysis of Ank2-L and Nrg180 protein levels in larval brain extracts of control and *CK2α* mutant animals. Ank2-L levels were slightly reduced in *CK2α*$^{P1/TikR}$ mutants. (L) Neuronal expression of Nrg in *CK2α*$^{P1/TikR}$ mutants failed to rescue the impairment in synapse stability (***, $P \leq 0.001$; $n = 9–15$ animals, muscles 1/9 and 2/10). n.s., not significant. Error bars represent SEM.

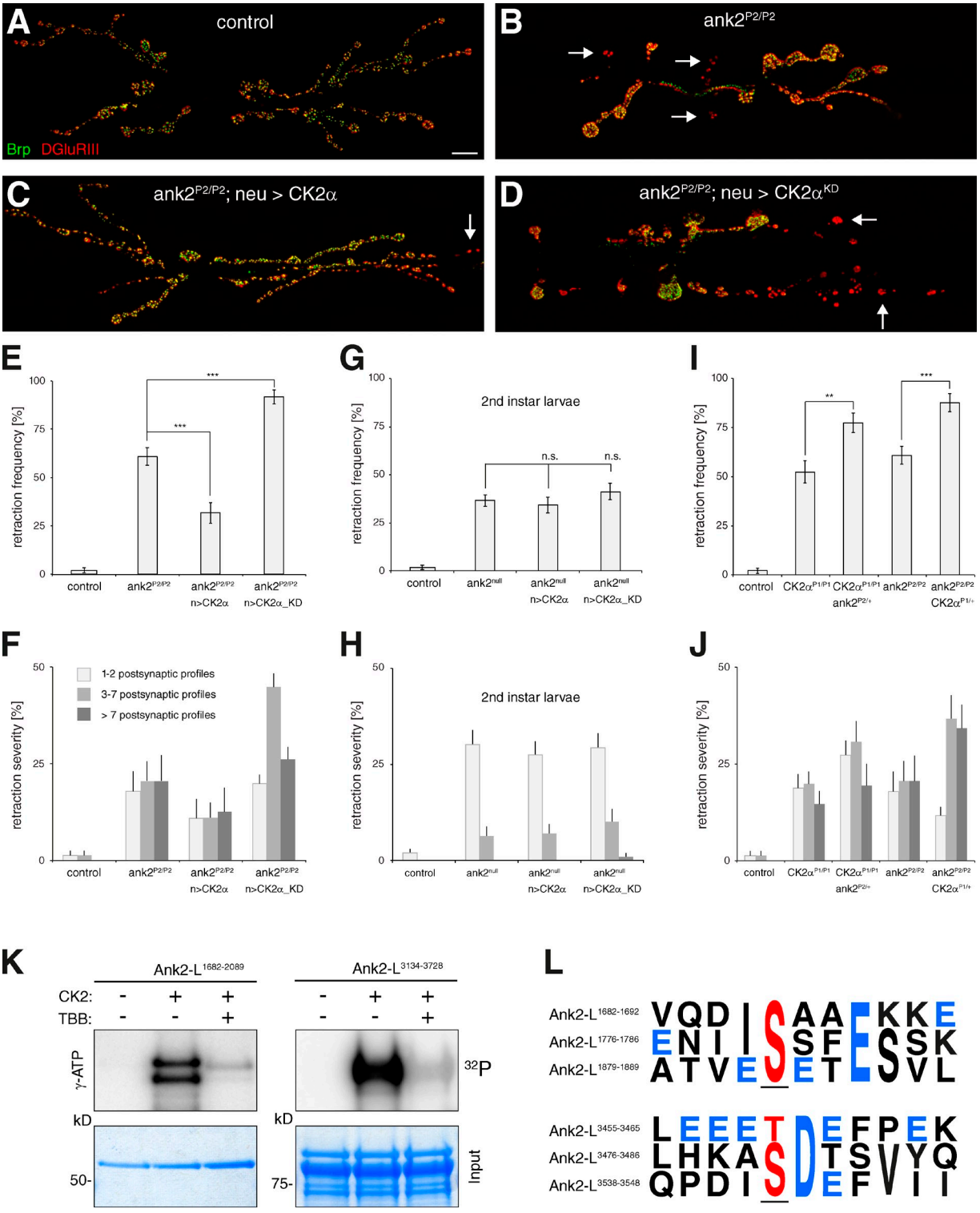

Figure 7. **CK2 controls synaptic stability via Ank2-L.** (A) A stable wild-type NMJ on muscles 6/7. (B) The hypomorphic *ank2*^{P2} mutation causes synaptic retractions (arrows). (C) Expression of wild-type CK2α in *ank2*$^{P2/P2}$ mutants significantly alleviated the synaptic retraction phenotype. (D) Expression of kinase-dead CK2α in *ank2*$^{P2/P2}$ mutants further enhanced the synaptic retraction phenotype. Bars, 10 µm. (E and F) Quantification of synaptic retraction frequency (E) and severity (F) for the genotypes described in A–D. (G and H) Quantification of synaptic retraction frequency (G) and severity (H) of second instar *ank2*$^{P1/P1}$-null mutant animals and *ank2*$^{P1/P1}$-null mutant animals expressing wild-type or kinase-dead CK2α. The *ank2*$^{P1/P1}$ phenotype was not significantly altered by CK2α expression. n.s., not significant. (I and J) Analysis of the genetic interaction between *CK2α* and *ank2-L*. Removal of one copy of *ank2-L* in *CK2α*$^{P1/P1}$ mutant animals or removal of one copy of *CK2α* in *ank2*$^{P2/P2}$ mutant animals significantly increased the frequency (I) and severity (J) of synaptic retractions compared with *CK2α*$^{P1/P1}$ and *ank2*$^{P2/P2}$ mutants, respectively (**, P ≤ 0.01; ***, P ≤ 0.001; *n* = 12–15 animals for E and F). (K) In vitro phosphorylation assays. Human CK2 phosphorylates purified Ank2-L protein domains (Ank2-L$^{1682–2089}$ = Ank2^{MT}; Ank2-L$^{3134–3728}$ = Ank2-L^{C}). Phosphorylation was inhibited in the presence of the CK2-specific inhibitor TBB. (L) Analysis of CK2-dependent phosphorylation of Ank2-L domains by mass spectrometry identified phosphorylated serine/threonine residues (red, underlined) in the Ank2^{MT} and Ank2-L^{C} domain. Examples of phosphorylation sites corresponding to the CK2 consensus motifs S/TXXE/D or S/TE/D are depicted. Acid residues are marked in blue. Error bars represent SEM.

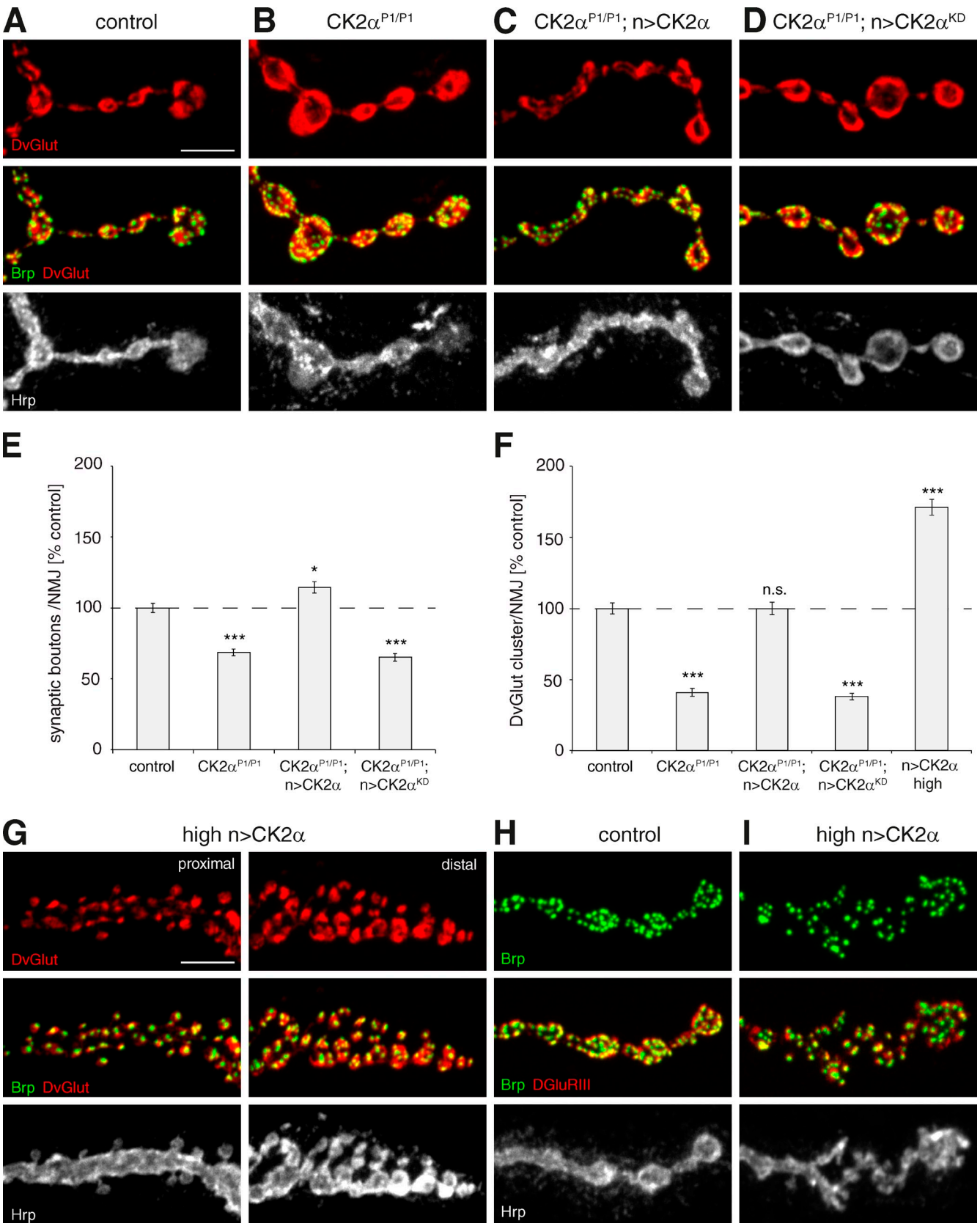

Figure 8. **CK2α controls synaptic bouton organization.** (A) At wild-type muscle 4 NMJs, synaptic vesicles (DvGlut, red) are clustered into distinct domains within individual synaptic boutons. (B) In *CK2α* mutants, synaptic vesicle domains were not organized into distinct clusters. (C and D) Presynaptic expression of wild-type (C) but not of kinase-dead CK2α (D) was sufficient to restore synaptic vesicle cluster organization. (E) Quantification of synaptic bouton number on muscle 4 (*, $P \leq 0.05$; ***, $P \leq 0.001$). (F) Quantification of the number of synaptic vesicle clusters per NMJ. Expression of wild-type but not of kinase-dead CK2α rescued the number of synaptic vesicle clusters. Overexpression of high levels of CK2α in wild-type animals caused a significant

potentially coordinate synapse stability (Pielage et al., 2008). We observed efficient phosphorylation of purified $Ank2^{MT}$ and Ank2-L^C proteins in vitro when using γ-ATP as a substrate for purified human CK2 (New England Biolabs, Inc.) that can be blocked by the addition of 30 µM of the CK2-specific inhibitor 4,5,6,7-tetrabromo-2-azabenzimidazole (TBB; Sarno et al., 2001; Fig. 7 K). We analyzed the reactions by mass spectroscopy and identified three residues in Ank^{MT} (S1686, S1780, and S1883) and six residues in Ank2-L^C (S3354, S3356, S3358, T3459, S3480, and S3542) that are efficiently phosphorylated by CK2 and are sensitive to the presence of the specific inhibitor TBB. These sites represent bona fide CK2 phosphorylation sites corresponding either to the S/TXXE/D (common in 90% of CK2 targets) or the S/TD/E (common in <10% CK2 targets) consensus sequence (Meggio and Pinna, 2003; Fig. 7 L). Together, these results identify Ank2 as a novel presynaptic CK2 target essential for the control of synaptic connectivity.

CK2 activity controls presynaptic organization

The reduced levels of Ank2-L and Futsch in *CK2* mutants raise the question of whether CK2 activity may not only be required for synapse stability but also for the organization of the presynaptic nerve terminal. Prior studies demonstrated that loss of Futsch results in fewer but larger synaptic boutons (Roos et al., 2000), whereas loss of Ank2-L perturbs the organization of synaptic vesicle domains (Pielage et al., 2008). In *CK2α* mutant animals we observed a 30% reduction in synaptic bouton number (Fig. 8, A, B, and E). In addition, synaptic vesicle domains that are clearly separated within boutons in control animals appear fused in *CK2α* mutant animals (Fig. 8, A, B, and F). The reduction in synaptic vesicle cluster number per NMJ was still significant when taking into account the concomitant reduction in NMJ size. Importantly, presynaptic expression of wild-type but not of kinase-dead *CK2α* was sufficient to rescue synaptic bouton number and vesicle organization (Fig. 8, C–F). Finally, we asked whether increased presynaptic CK2α activity might be sufficient to alter presynaptic organization. As CK2α activity correlates with CK2α protein levels in other systems (Trembley et al., 2009) we analyzed animals expressing increased *CK2α* levels (two copies of elav-GAL4, two copies of UAS-*CK2α*). In these animals, synaptic vesicle domains were subdivided into more numerous but smaller domains (Fig. 8, F and G), and we observed a dramatic increase in the number of satellite boutons per NMJ (control, 0.6 ± 0.19; high levels of CK2α, 20.45 ± 2.44 satellite boutons/muscle; 4 NMJ; $n = 20$ NMJs, 5 animals). These altered synaptic boutons often contained only a single synapse, a feature never observed at control NMJs (Fig. 8, G–I). Together, these results demonstrate that presynaptic CK2 activity is necessary and sufficient to control subcellular organization and stability of the presynaptic nerve terminal.

Discussion

The selective control of synapse maintenance is essential for the function and plasticity of neuronal circuits. Here, we provide evidence that synapse stability is actively controlled via posttranslational phosphorylation mechanisms. The systematic analysis of the kinome and phosphatome of *Drosophila* identified 11 kinases and phosphatases that are essential for the maintenance of synaptic connections. The genetic analysis of CK2α and CK2β using loss-of-function mutations enabled us to identify novel, essential requirements of CK2 in postmitotic neurons. Presynaptic CK2 activity is essential for synapse stability by controlling presynaptic localization of the adaptor molecule Ank2 that links synaptic cell adhesion molecules to the microtubule cytoskeleton. Constitutive phosphorylation-dependent regulation of the synaptic stability network provides a compelling mechanism to actively monitor and control the longevity of synaptic connections.

In our screen we identified phospholipid signaling (inositol kinase PI4KIIIα, inositol phosphatases CG9784 [IPP-like], Mipp2) metabolic signaling (IR, insulin receptor), and modulation of the presynaptic cytoskeleton (PP2A, PP4, cdc2, CKI, CK2, Mnb/Dyrk1a, Mast205) as important signaling nodes contributing to the control of synapse stability. These findings are consistent with prior implications of these pathways in synapse development and function (Di Paolo and De Camilli, 2006; Martín-Peña et al., 2006; Khuong et al., 2010; Cuesto et al., 2011; Frere et al., 2012). It is important to note that our screen likely did not identify the entire cellular signaling cascades controlling synapse maintenance. Low efficacies of individual RNAi lines (Dietzl et al., 2007) and potential redundant mechanisms may have prevented the identification of additional kinases and phosphatases contributing to synapse stability.

CK2 controls synapse stability

Despite indications for an important involvement of CK2 in neuronal development and function, the early embryonic lethality of CK2α and CK2β mutations in mice and *Drosophila* have thus far prevented detailed analysis of possible synaptic functions (Blanquet, 2000; Jauch et al., 2002; Lin et al., 2002; Buchou et al., 2003; Lou et al., 2008). Combinatorial genetic approaches using loss-of-function mutations enabled us to demonstrate that CK2α and CK2β are required within the presynaptic motoneuron to maintain synaptic connectivity.

Our in vivo rescue assays provided important novel insights into the molecular mechanisms regulating CK2 complex formation and function of individual subunits. We demonstrate that CK2β protein stability critically depends on the presence but not on the kinase activity of CK2α, whereas CK2α levels are less impacted by reductions in CK2β. The analysis of CK2β interaction sites of CK2α underscored the importance of using

1.7-fold increase in the number of DvGlut clusters compared with controls (***, $P \leq 0.001$; $n = 48$ NMJs). n.s., not significant. (G) Overexpression of CK2α significantly increases the number of satellite boutons and synaptic vesicle clusters. Small clusters of synaptic vesicles often associated with single presynaptic active zones (Brp, green). (H and I) In contrast to controls (H), synapses are no longer organized within uniformly sized synaptic boutons but separated within small satellite boutons (I). Bars, 5 µm. Error bars represent SEM.

in vivo assays for the analysis of relevant protein–protein interactions. In contrast to an in vitro study using a truncated version of CK2α (Raaf et al., 2011) and in contrast to our S2 cells' IP data, we demonstrated that only the $CK2\alpha^{L39*F52}$ double mutation but not the single mutations impair the CK2α–CK2β interaction or CK2 complex function in vivo. Interestingly, although not able to completely restore synapse stability or viability in CK2α mutants, this modified CK2α protein with minimal CK2β binding capacity provided slight alleviation of the synaptic retraction phenotype and slightly improved viability. This suggests that, at least under conditions where expression is artificially controlled, CK2α may have the potential to act independent of CK2β. In contrast, independent functions of CK2β in the nervous system are highly unlikely, as CKβ protein stability critically depended on a functional interaction with CK2α. We further demonstrate that a direct CK2α–PP2A interaction based on the previously described PP2A interaction motif (Hériché et al., 1997) is not necessary for the control of synapse stability. Together, our data indicate that CK2 primarily acts as a CK2α–CK2β complex in vivo while parallel, including PP2A-dependant, regulatory pathways also contribute to the control of synapse maintenance.

Our analysis of synapse retractions highlights two features that point toward mechanistic similarities with motor neuron diseases in vertebrates. Similar to heterogeneous vulnerabilities of different motor units in motor neuron diseases including amyotrophic lateral sclerosis and spinal muscular atrophy (Murray et al., 2010), we find that synapse stability is differentially affected at independent muscle groups. In addition, synapse retraction events were always initiated at terminal synaptic boutons (see, e.g., Fig. 2, E and F) resembling the dying back–like processes observed in several motoneuron and cognitive diseases (Saxena and Caroni, 2007).

CK2 controls presynaptic Ank2 localization and synapse organization

We have identified the adaptor protein Ank2-L as an important novel presynaptic target of CK2. We demonstrated that presynaptic localization of the L1-type CAM Nrg180, the adaptor protein Ank2-L, and of the MAP1b homologue Futsch critically depend on presynaptic CK2α activity. L1CAMs are direct targets of CK2 (Wong et al., 1996), and *Drosophila* Nrg is required for synapse stability (Enneking et al., 2013). However, although ectopic expression of Nrg180 partially restored presynaptic localization in *CK2α* mutant animals, it failed to restore presynaptic localization of Ank2-L or synapse stability. These results argue against Nrg180 as the primary synaptic target of CK2. Similarly, we can exclude the MAP1b Futsch as a causative target, as *futsch* loss-of-function mutations do not impair synapse stability (Eaton and Davis, 2005). In contrast, we present multiple lines of evidence that CK2 mediates synapse stability at least in part through the regulation of presynaptic Ank2-L localization. First, presynaptic Ank2-L distribution critically depended on CK2 kinase activity. Second, expression of CK2α significantly alleviated the synaptic retraction phenotype of *ank2-L* hypomorphic but not of *ank2* null mutations, which suggests that CK2 phosphorylation may enhance residual Ank2-L activity in these animals. Third, we observed a clear genetic interaction between *CK2α* and *ank2-L*. Finally, we demonstrated that CK2 phosphorylates several residues in the microtubule-binding and C-terminal domain of Ank2-L. Consistent with Ank2 being a prime target of CK2, Ank2-L is required for the maintenance of the synaptic localization of Nrg180, Futsch, and presynaptic microtubules (Koch et al., 2008; Pielage et al., 2008; Enneking et al., 2013). However, we cannot exclude the possibility that CK2 also controls parallel synapse stability pathways that in turn may affect the Ank2-L associated cytoskeleton.

The relevance of CK2 activity for cytoskeletal organization is underscored by the requirement of presynaptic CK2 activity for the subcellular organization of synaptic boutons. Decreased CK2 activity causes a reduction in synaptic bouton number and a loss of synaptic vesicle domain separation mimicking many phenotypic aspects of *futsch* and *ank2* mutants (Roos et al., 2000; Pielage et al., 2008). In contrast, increased CK2 activity results in an ectopic compartmentalization of the presynaptic terminal, with individual synapses often confined to small satellite boutons. Interestingly, a similar phenotype is caused by ectopic expression of the Ank2-L C terminus (Pielage et al., 2008). Modulation of presynaptic CK2 activity thus represents a potent mechanism to alter synaptic terminal organization and stability.

Regulation and relevance of synapse maintenance

The identification of CK2 as a constitutive active kinase raises the question of how synaptic stability is controlled in general. In principle, two modes of regulation can be envisioned. In one model, newly formed synapses are stable by default, and synapse elimination requires activation of signaling systems, selectively disrupting transsynaptic stability. In a second model, synapse stability requires constant posttranslational modifications of proteins essential for synapse maintenance. This would enable active surveillance of all stable synaptic connections and constitutes an elegant mechanism that immediately corrects inappropriate connectivity. Active stabilization mechanisms are consistent with the observation that in response to acquisition of new motor tasks only a very small number of newly formed synapses are selected for long-term stabilization (Xu et al., 2009; Yang et al., 2009; Fu et al., 2012). Interestingly, at rat hippocampal synapses, CK2 levels transiently increase in response to long-term potentiation, raising the possibility that activity-dependent signals may converge on synapse stability pathways (Charriaut-Marlangue et al., 1991). Combinatorial systems that actively control synapse stability and that also enable selective elimination of synapses would allow precise remodeling of neuronal circuits in response to developmental or activity-dependent signals. In support of active control of synapse stability, a recent live-imaging study demonstrated that it is not deficits in synapse formation that cause deficits in learning and memory associated with increased age and cognitive impairment but rather the selective failure to stabilize functional synaptic connections over time (Grillo et al., 2013).

Table 1. **Primers used in this study**

Primer	DNA sequence
CK2α pEntry N-term	5′-CACCATGACACTTCCTAGTG-3′
CK2α pEntry C-term	5′-TTATTGCTGATTATTGGGAT-3′
CK2β pEntry N-term	5′-CACCATGAGCAGCTCCGAGGAAG-3′
CK2β pEntry C-term	5′-TTAGTTTTTCGCTCGTAGTGG-3′
Site-directed mutagenesis	
CK2α K66M (kinase-dead)	5′-GGAAAAGTGCGTTGTTATGATTCTGAAACCTG-3′
CK2α L39A	5′-GCAATCAAGACGATTATCAGGCGGTCCGTAAATTAGGCCG-3′
CK2α F52A	5′-GTATTCTGAGGTCGCCGAGGCCATTAATATTACGACCACGG-3′
CK2α M161K	5′-GCATCGTGATGTAAAGCCCCACAATGTTAAGATAGATCACG-3′
CK2α E165D	5′-GTTATGATAGATCACGATAATCGAAAATTGCGCCTTATAG-3′
CK2α E165A	5′-GTTATGATAGATCACGCAAATCGAAAATTGCGCCTTATAG-3′
CK2α E165A R167A K168A	5′-GATAGATCACGCAAATGCAGCATTGCGCCTTATAG-3′

Materials and methods

Fly stocks

Flies were maintained at room temperature on standard food. All experiments were performed at 25°C unless otherwise indicated. The following fly strains were used in this study: w^{1118} (as wild type), *da*-Gal4 (Wodarz et al., 1995), *mef2*-Gal4, $elav^{C155}$-Gal4 (Lin and Goodman, 1994), BG*57*-Gal4 (Budnik et al., 1996), UAS-*mCD8-GFP*, P(hsFLP)86E, P(hsFLP)1, P(neoFRT)19A (Xu and Rubin, 1993), $CK2\alpha^{Tik}$, $CK2\alpha^{TikR}$ (Lin et al., 2002), $ank2^{f02001}$ ($ank2^{P2}$), $ank2^{f00518}$ ($ank2^{P1}$; Pielage et al., 2008), *dnMts* (Hannus et al., 2002), UAS-*dic2* (Dietzl et al., 2007), $CK2\beta^{MbuP1}$, $CK2\beta^{Mbu26\text{-}2}$ (Jauch et al., 2002), $CK2\alpha^{H3091}$, and $CK2\alpha^{G703}$ (Berger et al., 2008). PiggyBac insertions in *CK2α* were obtained from the Kyoto Stock Center: $CK2\alpha^{P1}$ (No. 141869, $PBac^{LL05896}$), $CK2\alpha^{P2}$ (No. 141994, $PBac^{LL07221}$; Schuldiner et al., 2008). RNAi stocks were ordered from the VDRC (Dietzl et al., 2007; listed in Table S1) or from the Bloomington Drosophila Stock Center: *CKIα* (No. 25786), *PP2A-29B* (No. 29384).

Generation of CK2α and CK2β constructs and transgenes

The ORFs of *CK2α* and *CK2β* were amplified by PCR from the cDNA plasmids LD27706 and RE31047 (Drosophila Genomic Research Center). Full-length ORFs were cloned into pENTR using TOPO cloning (Invitrogen) and shuffled into a pUASTattB-10×UAS destination vector with or without N-terminal 3×HA or EGFP tags (Enneking et al., 2013). Point mutations were introduced into pENTR clones using the QuikChange II site-directed mutagenesis kit (Agilent Technologies). Primers are listed in Table 1. Constructs were verified by sequencing (FMI Sequencing Facility). All constructs were injected into the attP40 genomic landing site using standard microinjection procedures (performed by ourselves or Genetic Services Inc.). Transgenic stocks were confirmed by sequencing (FMI Sequencing Facility).

Immunohistochemistry

Wandering third instar larvae were dissected in standard dissecting saline and fixed with Bouin's fixative for 2–5 min (Sigma-Aldrich). Primary antibodies were incubated overnight at 4°C and used at the following dilutions: anti-Brp (nc82) 1:250 (Wagh et al., 2006), anti-Synapsin (3c11) 1:50 (Klagges et al., 1996), anti-Nrg180 (BP104) 1:400 (Hortsch et al., 1990), rabbit anti-Dlg 1:30,000, rabbit anti-DGluRIII 1:2,500 (Pielage et al., 2011), rat anti-CD8 1:1,000 (Invitrogen), mouse anti-GFP (3E6) 1:1,000, rabbit anti-GFP (A6455) 1:2,000 (Invitrogen), rat anti-Ank2L 1:40 (Enneking et al., 2013), rabbit anti-CK2α 1:100 (raised against a peptide corresponding to aa 68–87 of *Drosophila* CK2α, AP22921PU-N; Acris). Alexa Fluor–conjugated secondary antibodies (Invitrogen) were used at 1:1,000 and applied for 2 h at room temperature. Alexa Fluor 488–, Alexa Fluor 647–, and Cy3-conjugated anti-HRP antibodies were used at 1:400–1,000 (Jackson ImmunoResearch Laboratories, Inc.). Images were captured using a confocal SPE microscope (Leica) with an HCX Plan Apochromat 63×/1.4 NA oil immersion objective lens at room temperature. For quantification of protein levels, all genotypes were imaged on the same day using identical settings for gain and offset. Imaris (Bitplane) and Photoshop (Adobe) were used for image processing and analysis.

CK2α and CK2β antibody production

For the generation of antibodies against *Drosophila* CK2α and CK2β, we generated N-terminal His_6-tagged full-length constructs using the pDEST17 vector (Invitrogen; primers are listed in Table 1). Both proteins were insoluble and were therefore purified under denaturing conditions using Spin-Trap columns according to the manufacturer's instructions (GE Healthcare). Polyclonal rabbit anti-CK2α and anti-CK2β antibodies were generated and purified at David's Biotechnologie.

Quantification of phenotypes

Synaptic retractions were quantified using presynaptic Brp and postsynaptic DGluRIII staining. Synapse retraction frequencies are presented as values per animal. For the determination of synaptic retraction severity, the numbers of unopposed postsynaptic bouton profiles per NMJ were counted. NMJs on the indicated muscle groups in segments A3–A6 were scored. *n* indicates the number of independent animals per quantification.

Presynaptic Nrg, Ank2-L, FasII, Futsch, and DvGlut levels were measured at distal, central, and proximal boutons of the presynaptic nerve terminal (segment A4 on muscle 4). The proximal bouton was defined as the first bouton after muscle innervation; the terminal bouton represented the distal bouton. Central boutons were at equal distances to proximal and distal boutons. Fluorescence intensity values were normalized to wild-type controls and quantified using Imaris (Bitplane).

Synaptic bouton number was quantified for type Ib boutons on muscle 4 (segments A2–A6) using Synapsin and Dlg staining. Satellite boutons were quantified on muscle 4 using Hrp staining (segments A4 and A5).

Western blot analysis and immunoprecipitation

Larval brains were dissected in HL3 saline in the presence of protease inhibitors (Roche), transferred into 2× sample buffer (Invitrogen), and boiled for 10 min at 95°C. Samples were run on 14% NuPage gels (Invitrogen) according to standard procedures. Gels were transferred to PVDF membrane for 2 h at 30 V, and membranes were probed with primary antibodies overnight at 4°C. Primary antibodies were used at the following concentrations: rabbit anti-CK2α 1:400, rabbit anti-CK2β 1:400, mouse anti-CK2β (6D5) 1:200 (EMD Millipore), mouse anti-Nrg^{BP104} (1:250), and mouse anti-tubulin (E7) 1:1,000 (Developmental Studies Hybridoma Bank). Secondary HRP-conjugated goat anti–mouse or goat anti–rabbit antibodies were used at 1:10,000 (Jackson ImmunoResearch Laboratories, Inc.) for 2 h at room temperature. Membranes were incubated with ECL substrate (SuperSignal West Pico kit; Thermo Fisher Scientific) and developed on film (Fujifilm).

For immunoprecipitation experiments, *Drosophila* S2 cells were cotransfected with *act5C*-Gal4, UAS-HA-CK2β, and one of the following plasmids: UAS-GFP, UAS-GFP-CK2α_wt, UAS-GFP-CK2α_KD, UAS-GFP-CK2α_L39A, UAS-GFP-CK2α_F52A, or UAS-GFP-CK2α_L39A_F52A. Fugene (Roche) was used as a transfection reagent according to the manufacturer's instructions. S2 cells were lysed using a TNT lysis buffer (300 mM NaCl, 50 mM Tris-HCL, pH 7.4, 1% Triton X-100, and 5 mM EDTA), incubated on ice for 30 min, and centrifuged for 10 min at 13,000 rpm and 4°C. GFP-TrapA beads (ChromoTek) were used to pull down GFP-CK2α according to the manufacturer's instructions. IPs were analyzed using mouse anti-HA (12CA5) 1:200, rabbit anti-GFP (Molecular Probes) 1:500, and mouse anti-tubulin 1:1,000.

MARCM analysis

The *CK2β*-null allele $CK2\beta^{26\text{-}2}$ was recombined onto the P(neoFRT)19A chromosome. The $CK2\beta^{26\text{-}2}$ P(neoFRT)19A stock was crossed to P(hsFLP)1, P(neoFRT)19A, tubGal80; *ok371*-Gal4, UAS-CD8-GFP; MKRS, P(hsFLP)86E.

Embryos were collected for 2 h and aged for an additional 3 h at 25°C. Embryos were heat shocked at 37.5°C for 1 h and kept overnight at 18°C before transfer to 25°C.

In vitro phosphorylation analysis

In vitro phosphorylation was performed by incubating 2.5 µg of purified $Ank2^{MT}$ or $Ank2\text{-}L^{C}$ protein with 250 U of human CK2 (New England Biolabs, Inc.) and 2 pmol γ-[^{32}P]ATP (3,000 Ci/mmol) for 30 min at 30°C in 50 µl 20 mM Tris, pH 7.5, 50 mM KCl, 10 mM $MgCl_2$, and 0.1 mM ATP. Where indicated, 30 µM of the CK2-specific inhibitor TBB was added to the reaction. For mass spectrometry analysis, the phosphorylation assays were conducted without γ-[^{32}P]ATP and precipitated with TCA.

Mass spectrometry

Protein pellets were dissolved in 0.5 M Tris, pH 8.6, and 6 M guanidinium hydrochloride, reduced in 16 mM TCEP for 30 min, and alkylated in 35 mM iodoacetamide for 30 min in the dark. The proteins were digested at 37°C with either trypsin (Promega) after 6× dilution in 50 mM Tris, 5 mM $CaCl_2$, pH 7.4, overnight, or Lys-C (Wako Chemicals USA) for 6 h after 3× dilution in 50 mM Tris and 5 mM CaCl2, pH 7.4, followed by trypsin overnight after an additional 2× dilution. Peptides were injected onto a reversed-phase column for liquid chromatography/tandem mass spectrometry analysis (LC-MS/MS) in the information-dependent acquisition mode. LC-MS/MS was performed using an Easy spray column (PepMap C18; 3 µm, 100 A, 75 µm × 15 cm) with an Easy-nLC 1000 high-performance liquid chromatograph system connected to a LTQ Orbitrap Velos equipped with an EasySpray source (Thermo Fisher Scientific). The peptides were loaded onto a peptide trap (Acclaim PepMap 100; Dionex) at a constant pressure of 500 bar. They were eluted at a flow rate of 300 nl/min with a linear gradient of 0–30% B in A in 10 min. A: 0.1% formic acid, 2% acetonitrile in water. B: 0.1% formic acid in acetonitrile. Information-dependent acquisition analyses were done according to the manufacturer's recommendations, i.e., one survey scan at 60,000 resolution in the Orbitrap cell was followed by up to 20 product ion scans in the linear ion trap, and precursors were excluded for 15 s after their second occurrence. Individual MS/MS spectra containing peptide sequence information were searched with the Mascot search engine (Matrix Science) against the Uniprot protein fasta sequence database (as of September 2012) or a custom database including the sequences of the expressed constructs. Carbamidomethylation of cysteine (+57.0245) was set as a fixed modification, and phosphorylation of serine and threonine (79.9663 D), oxidation of methionine (+15.9949 D), and acetylation of the protein N terminus (+42.0106 D) were set as variable modifications. Parent ion mass tolerance was set to 5 ppm and fragment ion mass tolerance to 0.6 D. The results were further validated with Scaffold and Scaffold PTM (Proteome Software). For phosphorylation site determination, the minimal localization probability was set to 95%.

Primers

See Table 1.

Statistical analysis

All statistical analyses were performed using a Student's two-tailed *t* test. Significant differences between compared genotypes are indicated (*, $P \leq 0.05$; **, $P \leq 0.01$; ***, $P \leq 0.001$).

Online supplemental material

Fig. S1 shows the analysis of synapse stability for the RNAi screen hits on muscle 4. Fig. S2 shows the analysis of synapse stability for the RNAi screens using independent pre- and postsynaptic markers. Fig. S3 describes the molecular nature of all CK2α mutations and shows the quantification of synaptic retraction frequency for all CK2α alleles on two different muscle groups. Fig. S4 shows the analysis of synaptic stability and formation phenotypes of PP2A mutant animals and the analysis of the presumptive CK2α-PP2A interaction. Table S1 lists all kinases and phosphatases and their VDRC number analyzed in the RNAi screen. Table S2 lists all data displayed in Figs. 1–8 and Figs. S1–S4. Online supplemental material is available at http://www.jcb.org/cgi/content/full/jcb.201305134/DC1.

We would like to thank T. Raabe, F.R. Jackson, T. Suzuki as well as the Bloomington Stock Center (Indiana), the Drosophila Genomics Research center (Indiana), the Kyoto Stock Center (Japan), the VDRC (Austria), and the Developmental Studies Hybridoma Bank (Iowa) for fly stocks, cDNAs, and antibodies. We thank D. Hess for the mass spectrometry analysis, E. Moreno for technical help, the FMI imaging and sequencing facilities for support, and all members of the Pielage laboratory for helpful discussions.

Research in the lab of J. Pielage was supported by the Swiss National Science Foundation and the Friedrich Miescher Institute for Biomedical Research.

Submitted: 27 May 2013
Accepted: 24 November 2013

References

Akten, B., E. Jauch, G.K. Genova, E.Y. Kim, I. Edery, T. Raabe, and F.R. Jackson. 2003. A role for CK2 in the *Drosophila* circadian oscillator. *Nat. Neurosci.* 6:251–257. http://dx.doi.org/10.1038/nn1007

Alvarez, V.A., and B.L. Sabatini. 2007. Anatomical and physiological plasticity of dendritic spines. *Annu. Rev. Neurosci.* 30:79–97. http://dx.doi.org/10.1146/annurev.neuro.30.051606.094222

Bednarek, E., and P. Caroni. 2011. β-Adducin is required for stable assembly of new synapses and improved memory upon environmental enrichment. *Neuron*. 69:1132–1146. http://dx.doi.org/10.1016/j.neuron.2011.02.034

Berger, J., K.A. Senti, G. Senti, T.P. Newsome, B. Asling, B.J. Dickson, and T. Suzuki. 2008. Systematic identification of genes that regulate neuronal wiring in the *Drosophila* visual system. *PLoS Genet.* 4:e1000085. http://dx.doi.org/10.1371/journal.pgen.1000085

Bischof, J., R.K. Maeda, M. Hediger, F. Karch, and K. Basler. 2007. An optimized transgenesis system for *Drosophila* using germ-line-specific phiC31 integrases. *Proc. Natl. Acad. Sci. USA*. 104:3312–3317. http://dx.doi.org/10.1073/pnas.0611511104

Blanquet, P.R. 2000. Casein kinase 2 as a potentially important enzyme in the nervous system. *Prog. Neurobiol.* 60:211–246. http://dx.doi.org/10.1016/S0301-0082(99)00026-X

Brachet, A., C. Leterrier, M. Irondelle, M.-P. Fache, V. Racine, J.-B. Sibarita, D. Choquet, and B. Dargent. 2010. Ankyrin G restricts ion channel diffusion at the axonal initial segment before the establishment of the diffusion barrier. *J. Cell Biol.* 191:383–395. http://dx.doi.org/10.1083/jcb.201003042

Bréchet, A., M.-P. Fache, A. Brachet, G. Ferracci, A. Baude, M. Irondelle, S. Pereira, C. Leterrier, and B. Dargent. 2008. Protein kinase CK2 contributes to the organization of sodium channels in axonal membranes by regulating their interactions with ankyrin G. *J. Cell Biol.* 183:1101–1114. http://dx.doi.org/10.1083/jcb.200805169

Buchou, T., M. Vernet, O. Blond, H.H. Jensen, H. Pointu, B.B. Olsen, C. Cochet, O.-G. Issinger, and B. Boldyreff. 2003. Disruption of the regulatory beta subunit of protein kinase CK2 in mice leads to a cell-autonomous defect and early embryonic lethality. *Mol. Cell. Biol.* 23:908–915. http://dx.doi.org/10.1128/MCB.23.3.908-915.2003

Budnik, V., Y.H. Koh, B. Guan, B. Hartmann, C. Hough, D. Woods, and M. Gorczyca. 1996. Regulation of synapse structure and function by the *Drosophila* tumor suppressor gene dlg. *Neuron*. 17:627–640. http://dx.doi.org/10.1016/S0896-6273(00)80196-8

Caroni, P., F. Donato, and D. Muller. 2012. Structural plasticity upon learning: regulation and functions. *Nat. Rev. Neurosci.* 13:478–490. http://dx.doi.org/10.1038/nrn3258

Charriaut-Marlangue, C., S. Otani, C. Creuzet, Y. Ben-Ari, and J. Loeb. 1991. Rapid activation of hippocampal casein kinase II during long-term potentiation. *Proc. Natl. Acad. Sci. USA*. 88:10232–10236. http://dx.doi.org/10.1073/pnas.88.22.10232

Cheusova, T., M.A. Khan, S.W. Schubert, A.-C. Gavin, T. Buchou, G. Jacob, H. Sticht, J. Allende, B. Boldyreff, H.R. Brenner, and S. Hashemolhosseini. 2006. Casein kinase 2-dependent serine phosphorylation of MuSK regulates acetylcholine receptor aggregation at the neuromuscular junction. *Genes Dev.* 20:1800–1816. http://dx.doi.org/10.1101/gad.375206

Chung, H.J., Y.H. Huang, L.-F. Lau, and R.L. Huganir. 2004. Regulation of the NMDA receptor complex and trafficking by activity-dependent phosphorylation of the NR2B subunit PDZ ligand. *J. Neurosci.* 24:10248–10259. http://dx.doi.org/10.1523/JNEUROSCI.0546-04.2004

Cuesto, G., L. Enriquez-Barreto, C. Caramés, M. Cantarero, X. Gasull, C. Sandi, A. Ferrús, A. Acebes, and M. Morales. 2011. Phosphoinositide-3-kinase activation controls synaptogenesis and spinogenesis in hippocampal neurons. *J. Neurosci.* 31:2721–2733. http://dx.doi.org/10.1523/JNEUROSCI.4477-10.2011

Dietzl, G., D. Chen, F. Schnorrer, K.C. Su, Y. Barinova, M. Fellner, B. Gasser, K. Kinsey, S. Oppel, S. Scheiblauer, et al. 2007. A genome-wide transgenic RNAi library for conditional gene inactivation in *Drosophila*. *Nature*. 448:151–156. http://dx.doi.org/10.1038/nature05954

Di Paolo, G., and P. De Camilli. 2006. Phosphoinositides in cell regulation and membrane dynamics. *Nature*. 443:651–657. http://dx.doi.org/10.1038/nature05185

Eaton, B.A., and G.W. Davis. 2005. LIM Kinase1 controls synaptic stability downstream of the type II BMP receptor. *Neuron*. 47:695–708. http://dx.doi.org/10.1016/j.neuron.2005.08.010

Eaton, B.A., R.D. Fetter, and G.W. Davis. 2002. Dynactin is necessary for synapse stabilization. *Neuron*. 34:729–741. http://dx.doi.org/10.1016/S0896-6273(02)00721-3

Enneking, E.-M., S.R. Kudumala, E. Moreno, R. Stephan, J. Boerner, T.A. Godenschwege, and J. Pielage. 2013. Transsynaptic coordination of synaptic growth, function, and stability by the L1-type CAM Neuroglian. *PLoS Biol.* 11:e1001537. http://dx.doi.org/10.1371/journal.pbio.1001537

Frere, S.G., B. Chang-Ileto, and G. Di Paolo. 2012. Role of phosphoinositides at the neuronal synapse. *Subcell. Biochem.* 59:131–175. http://dx.doi.org/10.1007/978-94-007-3015-1_5

Fu, M., X. Yu, J. Lu, and Y. Zuo. 2012. Repetitive motor learning induces coordinated formation of clustered dendritic spines in vivo. *Nature*. 483:92–95. http://dx.doi.org/10.1038/nature10844

Grillo, F.W., S. Song, L.M. Teles-Grilo Ruivo, L. Huang, G. Gao, G.W. Knott, B. Maco, V. Ferretti, D. Thompson, G.E. Little, and V. De Paola. 2013. Increased axonal bouton dynamics in the aging mouse cortex. *Proc. Natl. Acad. Sci. USA*. 110:E1514–E1523. http://dx.doi.org/10.1073/pnas.1218731110

Hafezparast, M., R. Klocke, C. Ruhrberg, A. Marquardt, A. Ahmad-Annuar, S. Bowen, G. Lalli, A.S. Witherden, H. Hummerich, S. Nicholson, et al. 2003. Mutations in dynein link motor neuron degeneration to defects in retrograde transport. *Science*. 300:808–812. http://dx.doi.org/10.1126/science.1083129

Hannus, M., F. Feiguin, C.P. Heisenberg, and S. Eaton. 2002. Planar cell polarization requires Widerborst, a B' regulatory subunit of protein phosphatase 2A. *Development*. 129:3493–3503.

Hériché, J.K., F. Lebrin, T. Rabilloud, D. Leroy, E.M. Chambaz, and Y. Goldberg. 1997. Regulation of protein phosphatase 2A by direct interaction with casein kinase 2alpha. *Science*. 276:952–955. http://dx.doi.org/10.1126/science.276.5314.952

Holtmaat, A., and K. Svoboda. 2009. Experience-dependent structural synaptic plasticity in the mammalian brain. *Nat. Rev. Neurosci.* 10:647–658. http://dx.doi.org/10.1038/nrn2699

Hortsch, M., A.J. Bieber, N.H. Patel, and C.S. Goodman. 1990. Differential splicing generates a nervous system-specific form of *Drosophila* neuroglian. *Neuron*. 4:697–709. http://dx.doi.org/10.1016/0896-6273(90)90196-M

Huang, H.-D., T.-Y. Lee, S.-W. Tzeng, and J.-T. Horng. 2005. KinasePhos: a web tool for identifying protein kinase-specific phosphorylation sites. *Nucleic Acids Res.* 33(Web Server issue):W226–W229. http://dx.doi.org/10.1093/nar/gki471

Huillard, E., L. Ziercher, O. Blond, M. Wong, J.-C. Deloulme, S. Souchelnytskyi, J. Baudier, C. Cochet, and T. Buchou. 2010. Disruption of CK2beta in embryonic neural stem cells compromises proliferation and oligodendrogenesis in the mouse telencephalon. *Mol. Cell. Biol.* 30:2737–2749. http://dx.doi.org/10.1128/MCB.01566-09

Ikeda, Y., K.A. Dick, M.R. Weatherspoon, D. Gincel, K.R. Armbrust, J.C. Dalton, G. Stevanin, A. Dürr, C. Zühlke, K. Bürk, et al. 2006. Spectrin mutations cause spinocerebellar ataxia type 5. *Nat. Genet.* 38:184–190. http://dx.doi.org/10.1038/ng1728

Jauch, E., J. Melzig, M. Brkulj, and T. Raabe. 2002. In vivo functional analysis of *Drosophila* protein kinase casein kinase 2 (CK2) beta-subunit. *Gene*. 298:29–39. http://dx.doi.org/10.1016/S0378-1119(02)00921-6

Jenkins, S.M., and V. Bennett. 2001. Ankyrin-G coordinates assembly of the spectrin-based membrane skeleton, voltage-gated sodium channels, and L1 CAMs at Purkinje neuron initial segments. *J. Cell Biol.* 155:739–746. http://dx.doi.org/10.1083/jcb.200109026

Khuong, T.M., R.L. Habets, J.R. Slabbaert, and P. Verstreken. 2010. WASP is activated by phosphatidylinositol-4,5-bisphosphate to restrict synapse growth in a pathway parallel to bone morphogenetic protein signaling. *Proc. Natl. Acad. Sci. USA*. 107:17379–17384. http://dx.doi.org/10.1073/pnas.1001794107

Klagges, B.R., G. Heimbeck, T.A. Godenschwege, A. Hofbauer, G.O. Pflugfelder, R. Reifegerste, D. Reisch, M. Schaupp, S. Buchner, and E. Buchner. 1996. Invertebrate synapsins: a single gene codes for several isoforms in *Drosophila*. *J. Neurosci.* 16:3154–3165.

Koch, I., H. Schwarz, D. Beuchle, B. Goellner, M. Langegger, and H. Aberle. 2008. *Drosophila* ankyrin 2 is required for synaptic stability. *Neuron*. 58:210–222. http://dx.doi.org/10.1016/j.neuron.2008.03.019

Lee, T., and L. Luo. 1999. Mosaic analysis with a repressible cell marker for studies of gene function in neuronal morphogenesis. *Neuron*. 22:451–461. http://dx.doi.org/10.1016/S0896-6273(00)80701-1

Lin, D.M., and C.S. Goodman. 1994. Ectopic and increased expression of Fasciclin II alters motoneuron growth cone guidance. *Neuron*. 13:507–523. http://dx.doi.org/10.1016/0896-6273(94)90022-1

Lin, J.-M., V.L. Kilman, K. Keegan, B. Paddock, M. Emery-Le, M. Rosbash, and R. Allada. 2002. A role for casein kinase 2alpha in the *Drosophila* circadian clock. *Nature*. 420:816–820. http://dx.doi.org/10.1038/nature01235

Litchfield, D.W. 2003. Protein kinase CK2: structure, regulation and role in cellular decisions of life and death. *Biochem. J.* 369:1–15. http://dx.doi.org/10.1042/BJ20021469

Lou, D.Y., I. Dominguez, P. Toselli, E. Landesman-Bollag, C. O'Brien, and D.C. Seldin. 2008. The alpha catalytic subunit of protein kinase CK2 is required for mouse embryonic development. *Mol. Cell. Biol.* 28:131–139. http://dx.doi.org/10.1128/MCB.01119-07

Martín-Peña, A., A. Acebes, J.-R. Rodríguez, A. Sorribes, G.G. de Polavieja, P. Fernández-Fúnez, and A. Ferrús. 2006. Age-independent synaptogenesis by phosphoinositide 3 kinase. *J. Neurosci.* 26:10199–10208. http://dx.doi.org/10.1523/JNEUROSCI.1223-06.2006

Meggio, F., and L.A. Pinna. 2003. One-thousand-and-one substrates of protein kinase CK2? *FASEB J.* 17:349–368. http://dx.doi.org/10.1096/fj.02-0473rev

Murray, L.M., K. Talbot, and T.H. Gillingwater. 2010. Review: neuromuscular synaptic vulnerability in motor neurone disease: amyotrophic lateral sclerosis and spinal muscular atrophy. *Neuropathol. Appl. Neurobiol.* 36:133–156.

Niefind, K., J. Raaf, and O.-G. Issinger. 2009. Protein kinase CK2 in health and disease: Protein kinase CK2: from structures to insights. *Cell. Mol. Life Sci.* 66:1800–1816. http://dx.doi.org/10.1007/s00018-009-9149-8

Penner, C.G., Z. Wang, and D.W. Litchfield. 1997. Expression and localization of epitope-tagged protein kinase CK2. *J. Cell. Biochem.* 64:525–537. http://dx.doi.org/10.1002/(SICI)1097-4644(19970315)64:4<525::AID-JCB13.0.CO;2-T

Pielage, J., R.D. Fetter, and G.W. Davis. 2005. Presynaptic spectrin is essential for synapse stabilization. *Curr. Biol.* 15:918–928. http://dx.doi.org/10.1016/j.cub.2005.04.030

Pielage, J., L. Cheng, R.D. Fetter, P.M. Carlton, J.W. Sedat, and G.W. Davis. 2008. A presynaptic giant ankyrin stabilizes the NMJ through regulation of presynaptic microtubules and transsynaptic cell adhesion. *Neuron*. 58:195–209. http://dx.doi.org/10.1016/j.neuron.2008.02.017

Pielage, J., V. Bulat, J.B. Zuchero, R.D. Fetter, and G.W. Davis. 2011. Hts/Adducin controls synaptic elaboration and elimination. *Neuron*. 69:1114–1131. http://dx.doi.org/10.1016/j.neuron.2011.02.007

Raaf, J., N. Bischoff, K. Klopffleisch, E. Brunstein, B.B. Olsen, G. Vilk, D.W. Litchfield, O.-G. Issinger, and K. Niefind. 2011. Interaction between CK2α and CK2β, the subunits of protein kinase CK2: thermodynamic contributions of key residues on the CK2α surface. *Biochemistry*. 50:512–522. http://dx.doi.org/10.1021/bi1013563

Roos, J., T. Hummel, N. Ng, C. Klämbt, and G.W. Davis. 2000. *Drosophila* Futsch regulates synaptic microtubule organization and is necessary for synaptic growth. *Neuron*. 26:371–382. http://dx.doi.org/10.1016/S0896-6273(00)81170-8

Salvi, M., S. Sarno, O. Marin, F. Meggio, E. Itarte, and L.A. Pinna. 2006. Discrimination between the activity of protein kinase CK2 holoenzyme and its catalytic subunits. *FEBS Lett.* 580:3948–3952. http://dx.doi.org/10.1016/j.febslet.2006.06.031

Sanz-Clemente, A., J.A. Matta, J.T.R. Isaac, and K.W. Roche. 2010. Casein kinase 2 regulates the NR2 subunit composition of synaptic NMDA receptors. *Neuron*. 67:984–996. http://dx.doi.org/10.1016/j.neuron.2010.08.011

Sarno, S., H. Reddy, F. Meggio, M. Ruzzene, S.P. Davies, A. Donella-Deana, D. Shugar, and L.A. Pinna. 2001. Selectivity of 4,5,6,7-tetrabromobenzotriazole, an ATP site-directed inhibitor of protein kinase CK2 ('casein kinase-2'). *FEBS Lett.* 496:44–48. http://dx.doi.org/10.1016/S0014-5793(01)02404-8

Saxena, S., and P. Caroni. 2007. Mechanisms of axon degeneration: from development to disease. *Prog. Neurobiol.* 83:174–191. http://dx.doi.org/10.1016/j.pneurobio.2007.07.007

Saxena, A., R. Padmanabha, and C.V. Glover. 1987. Isolation and sequencing of cDNA clones encoding alpha and beta subunits of *Drosophila melanogaster* casein kinase II. *Mol. Cell. Biol.* 7:3409–3417.

Schuldiner, O., D. Berdnik, J.M. Levy, J.S. Wu, D. Luginbuhl, A.C. Gontang, and L. Luo. 2008. piggyBac-based mosaic screen identifies a postmitotic function for cohesin in regulating developmental axon pruning. *Dev. Cell*. 14:227–238. http://dx.doi.org/10.1016/j.devcel.2007.11.001

Schuster, C.M., G.W. Davis, R.D. Fetter, and C.S. Goodman. 1996. Genetic dissection of structural and functional components of synaptic plasticity. I. Fasciclin II controls synaptic stabilization and growth. *Neuron*. 17:641–654. http://dx.doi.org/10.1016/S0896-6273(00)80197-X

Seldin, D.C., D.Y. Lou, P. Toselli, E. Landesman-Bollag, and I. Dominguez. 2008. Gene targeting of CK2 catalytic subunits. *Mol. Cell. Biochem.* 316:141–147. http://dx.doi.org/10.1007/s11010-008-9811-8

Trembley, J.H., G. Wang, G. Unger, J. Slaton, and K. Ahmed. 2009. Protein kinase CK2 in health and disease: CK2: a key player in cancer biology. *Cell. Mol. Life Sci.* 66:1858–1867.

Viquez, N.M., P. Füger, V. Valakh, R.W. Daniels, T.M. Rasse, and A. DiAntonio. 2009. PP2A and GSK-3beta act antagonistically to regulate active zone development. *J. Neurosci.* 29:11484–11494. http://dx.doi.org/10.1523/JNEUROSCI.5584-08.2009

Wagh, D.A., T.M. Rasse, E. Asan, A. Hofbauer, I. Schwenkert, H. Dürrbeck, S. Buchner, M.C. Dabauvalle, M. Schmidt, G. Qin, et al. 2006. Bruchpilot, a protein with homology to ELKS/CAST, is required for structural integrity and function of synaptic active zones in *Drosophila*. *Neuron*. 49:833–844. http://dx.doi.org/10.1016/j.neuron.2006.02.008

Wodarz, A., U. Hinz, M. Engelbert, and E. Knust. 1995. Expression of crumbs confers apical character on plasma membrane domains of ectodermal epithelia of *Drosophila*. *Cell*. 82:67–76. http://dx.doi.org/10.1016/0092-8674(95)90053-5

Wong, E.V., A.W. Schaefer, G. Landreth, and V. Lemmon. 1996. Casein kinase II phosphorylates the neural cell adhesion molecule L1. *J. Neurochem.* 66:779–786. http://dx.doi.org/10.1046/j.1471-4159.1996.66020779.x

Xu, T., and G.M. Rubin. 1993. Analysis of genetic mosaics in developing and adult Drosophila tissues. *Development*. 117:1223–1237.

Xu, T., X. Yu, A.J. Perlik, W.F. Tobin, J.A. Zweig, K. Tennant, T. Jones, and Y. Zuo. 2009. Rapid formation and selective stabilization of synapses for enduring motor memories. *Nature*. 462:915–919. http://dx.doi.org/10.1038/nature08389

Yang, G., F. Pan, and W.-B. Gan. 2009. Stably maintained dendritic spines are associated with lifelong memories. *Nature*. 462:920–924. http://dx.doi.org/10.1038/nature08577